FINAL TECHNICAL REPORT
U.S. Geological Survey
National Earthquake Hazards Reduction Program

Award No. G10AC00686
Start date: Sept. 14, 2010; End date: March 13, 2012

Title of Award:

Investigations of deformation of the Columbia River basalt and younger sediments in the vicinity of the Yakima River canyon

Recipient:

Harvey M. Kelsey
Department of Geology
Humboldt State University
Arcata, CA 95521

Title of Technical Report:

LATE QUATERNARY LANDSCAPE EVOLUTION AND DEFORMATION IN THE FORELIMB REGION OF THE MANASTASH ANTICLINE, YAKIMA FOLD BELT, WASHINGTON

Authors of Technical Report:

Tyler C. Ladinsky
Department of Geology
Humboldt State University
Arcata, Ca 95521
ty.ladinsky@gmail.com
831 239 9675

Harvey M. Kelsey
Department of Geology
Humboldt State University
Arcata, CA 95521
hmk1@humboldt.edu
707 826-3991

LATE QUATERNARY LANDSCAPE EVOLUTION AND DEFORMATION IN THE FORELIMB REGION OF THE MANASTASH ANTICLINE, YAKIMA FOLD BELT, WASHINGTON

ABSTRACT

Using the forelimb of an anticline within the Yakima Fold Belt, Washington, as a case study, we investigate the Quaternary evolution of a range front that juxtaposes an actively growing anticlinal ridge with an adjacent basin. The forelimb of the Manastash anticline forms the range front that delineates the Manastash Range from the Kittitas Valley to the north. At the Kittitas Valley-range front junction, two different geomorphic settings occur. The two settings contrast, in one case, a range front that is the site of active thrust faulting (west-of-canyon range front) with, in the other case, a range front (east-of-canyon range front) where the active fault is buried and blind and the range front morphology is unaffected by active tectonics. For the west-of-canyon range front, both youthful fault scarps and faults that are apparent on a seismic reflection profile provide evidence that the range front is separated from the adjoining Kittitas Valley to the north by active reverse faults. Based on knickpoints in tributaries and preserved late Quaternary uplifted alluvial fan remnants in the same tributaries, we infer that slip on the range front fault system has uplifted Manastash Ridge and tightened the Manastash anticline in late Quaternary time. Alluvial fans bound the range front; and, based on luminescence ages on these fans, we infer that fan building episodes are most vigorous in interglacial periods and fans are entrenched in colder climate periods. Because sequences of fans are vertically separated by fault scarps on that portion of the range front with active frontal faults, we infer that fans, while constructed during favorable interglacial climate regimes, are elevated and entrenched within the range front as a consequence of periodic earthquakes on south-dipping ramp thrusts that underlie the Manastash Ridge and Manastash anticline.

INTRODUCTION

The Yakima fold belt (YFB) is an extensive structural sub-province within south central Washington (Figure 1) primarily composed of west trending, north verging, narrow anticlinal ridges and broad synclinal valleys (Bentley, 1977; Reidel 1984). The Yakima fold belt covers approximately 14,000 km^2 and encompasses the western portion of the Columbia Plateau (Reidel et al., 1994; Tolan et al., 2009). Anticlinal ridges vary in length from 1 km to >200 km and fold wavelength varies from 3 to 20 km (Tolan et al., 2009). Typically, exposed geometry of major anticlines is asymmetrical with a steeply dipping northern limb (Tolan et al., 2009; Reidel et al., 1994). Secondary folding and faulting is common within the steep forelimb (Price et al., 1989)

Deformation of the Columbia River basalt commenced during emplacement because the oldest basalt group (Grande Ronde) thins over anticlinal ridges (Reidel, 1984), and facies trends in sediments intercalated with the basalt record growth of the folds in the middle Miocene and Pliocene (Smith, 1998). Geophysical data indicate basement units have undergone greater amount of shortening than the overlying Columbia River Basalt Group, suggesting folding was active prior as well as during the emplacement of the basalt flows (Blakely et al., 2011). Deformation in the fold belt is ongoing because several folds in the Yakima fold belt are associated with active faults that have Holocene scarps (Campbell and Bentley, 1981; West et al., 1996).

Although the age and magnetostratigraphy of the basalt is reasonably well established, deformation rates and style over the time span since the basalt has been emplaced remain unclear. At one extreme, the anticlinal ridges that make up the Yakima fold belt largely could be topographic expressions of folds developed in Tertiary time. Conversely, the folds largely could be constructional topographic landforms and these actively growing folds create the modern expression of the Yakima Fold Belt. Reidel et al. (1994) and Tolan et al. (2009) suggest that the majority of the present structural relief has been generated since cessation of the last major basalt (Elephant Mountain member) outpouring at 10.5 Ma.

This report addresses the following three related hypotheses: first, individual anticlines of the Yakima Fold Belt are actively growing folds; second, thrust (or reverse) faulting is the driving mechanism for folding and the folds are hanging wall anticlines in the upper plate of the thrusts; and third, thrust faults daylight at the range front. These hypotheses form the basis for the research approach and data collection.

These hypotheses are evaluated by selecting a range front of an anticline within the Yakima Fold Belt. We address the geomorphic and tectonic evolution of the Manastash range front, which provides insight into the structural growth and evolution of the Manastash anticline. The Manastash range front is the range front of Manasatash Ridge (Figure 2); and the ridge is the topographic expression of the Manastash anticline, which is a northeast-trending fold within the fold belt. According to Reidel et al. (1994), the maximum structural relief of the Manastash anticline is 380 m.

The valley bottom-to-upland transition between Kittitas Valley and the Manasatash Ridge to the south (Figures 2 and 3) is the focus of our field investigations. We map the Quaternary deposits and evaluate whether late-Quaternary-age structures have deformed or uplifted sediment along the range front. Our investigations entail geologic mapping, geochronology of Quaternary units, geomorphic/neo-tectonic mapping on LiDAR imagery, morphometric analyses of digital elevation models (DEMs), and incorporation of seismic reflection data across the range front.

RESEARCH APPROACH

A geologic map was constructed along the Manastash range front using a suite of techniques including compilation of existing geologic maps (Washington Department of Natural Resources, 1978), analysis of LiDAR imagery, inventory of alluvial clast characteristics and field mapping. The fieldwork focused primarily on mapping Quaternary surficial units. However, we collected bedding attitudes in the Tertiary basalt and sedimentary facies in order to reevaluate the structure of the Manastash anticline.

One of the goals of the geologic investigation was to distinguish, using an approach introduced by Waitt (1979), Yakima River (mainstream) cobble lithofacies from locally derived (sidestream) gravels. Alluvial clasts were inventoried from five different outcrops that were chosen to represent distinct Quaternary lithofacies. To avoid over sampling units with less aerial extent, the sampling method was scaled to outcrop exposure. We collected 10 pebbles and/or cobbles per meter of outcrop to note lithology, diameter, roundness, and rind thickness. The minimum and maximum sample population was 60 and 110 respectively. Clast lithology was categorized into Columbia River Basalt Group (CRBG), Cascade Volcanics, and Other; clast lithology and degree of clast roundness were the best criteria for distinguishing the alluvial lithofacies.

Age evaluation for the surficial units employed both relative age assessment using geomorphic, geospatial, and stratigraphic relationships as well as age estimates based on

microprobe tephra analyses and infrared stimulated luminescence analyses. A tephra sample was analyzed by the United States Geological Survey Tephrochronology Lab in Menlo Park, California. Infrared stimulated luminescence analyses were performed on six loess and alluvial samples by the United States Geological Survey Luminescence Dating Laboratory in Denver, Colorado. Relative dating assessments, tephrochronology, and infrared stimulated luminescence analyses together provide a set of criteria for estimating ages of the Quaternary units and assessing the timing of deformation of the Manastash anticline.

We also incorporated previous age estimates for the Thorp gravel, which is an extensive alluvial unit in the northern and western portion of the Kittatas valley upstream of the Mansatash range front. Fission track dating of tephra airfall deposits constrained the Thorp Gravels to be 3.7 my (Pliocene) in age (Porter, 1976; Waitt, 1979). Due to lack of stratigraphic continuity and indistinct geomorphic relationships between the northern and southern Kittitas Valley, it is unclear if the older surficial units within the study area are contemporaneous with the Thorp Gravel as mapped by Waitt (1979). However, Bentley (1977) mapped Thorp Gravel overlying Miocene Ellensburg sediment at Potato Hill. Potato Hill is an erosional remnant in the southern Kittitas valley (Figure 3).

Acquisition of high-resolution (1 m) light detection and ranging (LiDAR) imagery for the Manastash Ridge and southern Kittitas Valley allowed documentation of Quaternary surfaces and fault lineaments along the northern Manastash range front. The LiDAR data set, collected by the Army Yakima Training Center, consists of 1 m postings projected into UTM Zone 10 NAD83 coordinate system. LiDAR survey accuracy is equivalent to 8 pulses/m^2.

Longitudinal profiles of Manastash range front tributaries were extracted from the 1 m LiDAR imagery. The one exception was Shushuskin canyon (Figure 3). Because Shushuskin Canyon extended beyond the boundary of the LiDAR data set, the Shushuskin Canyon channel profile was extracted using 10 m digital elevation model (DEM) imagery. For all tributaries, extraction of the raw data was facilitated through Matlab and ArcGIS as outlined by geomorphtools.org (Whipple et al., 2007). The raw stream gradient and drainage area data were log-transformed and the resultant slope-area plots were used to determine the channel concavity (θ). Longitudinal profiles of tributaries were analyzed in order to document knickpoints along the range front. Compilation of knickpoint and concavity data served as a basis to delineate changes in baselevel along the range front (Kirby et al, 2001, Snyder et al., 2000, Wobus et al., 2006). The majority of tributaries within the east-of-the-canyon range front were anthropogenically influenced by highway 82, making the steep headwaters segmented from the lower reaches. We attempted to mitigate the influence of the highway by choosing tributaries with the most continuous channel profiles.

The United States Geological Survey (USGS) provided access to a 3 km long seismic reflection line along Umtanum Road, which extends from the Kittitas Valley floor southwest into Shushuskin Canyon. The data were collected (T. Pratt, written communication, July 15, 2012) on 216 receiver channels with 5-m source and receiver spacing using a vibroseis seismic source (12-sec sweeps, 20-160 Hz frequencies). Standard CMP processing was employed. Detailed geologic mapping within the vicinity of the seismic reflection line enabled a composite structural interpretation of the geometry of the Manastash range front and fault system.

RESULTS

Pebble and Cobble Data for Tertiary and Quaternary Units

Histograms of pebble lithology and pebble roundness from five different localities, four Quaternary units and a Miocene Ellensburg Formation conglomerate, document the composition of the surficial units (Figure 4). Modern Yakima River and paleo-Yakima River deposits had significantly different percentages of Columbia River Basalt Group (CRBG) clasts with modern alluvium having 44% CRBG and the paleo-Yakima River alluvium having 75% CRBG clasts (Figure 4). Degree of roundness further differentiated modern and paleo-Yakima River alluvium. The modern Yakima facies has predominately rounded (35%) and sub-rounded (32%) pebbles while the paleo-Yakima facies were predominately sub-rounded (33%) and sub-angular (29%).

Both Spring Canyon and Shushuskin Canyon fan deposits yield an identical lithologic composition of 100% Columbia River Basalt Group (CRBG). Dominate pebble roundness varied slightly between angular and sub-angular for both localities with respective values of 44% and 33% for Spring Canyon 36% and 43% for Shushuskin Canyon.

Pebble lithology and pebble roundness for the Miocene Ellensburg Formation conglomerate facies are distinct from the Quaternary facies (Figure 4). For the Miocene conglomerate, the dominate clast is a rounded (43%) Cascade volcanic clast (62%).

Quaternary Alluvium Units of the Manastash Range Front

Geologic mapping focused on identifying surficial units that document the transition from the topographic highland to the Yakima River floodplain at the south end of the Kittitas Valley. The Quaternary units consist of alluvial deposits of the Yakima River watershed that include detritus sourced in the Cascade Range and tributary alluvial deposits that are sourced in the Columbia River Basalt Group of the Manastash Ridge within the Yakima Fold Belt (Figure 5). Yakima River alluvial deposits include both modern alluvium and terrace deposits that are now elevated above the Yakima River floodplain.

The tributary alluvium aggraded as fan deposits along the range front or within the lower reaches of tributaries that debouch onto the floodplain of the Yakima River. The alluvial fan deposits are separated into seven units of increasing relative age based on elevation and degree of preservation of fan morphology (Figure 5). Loess deposits of varying thickness and degrees of cementation cap fan surfaces. Loess deposits were noted in the field but not differentiated by relative age (Figure 5). Mapping loess by relative thickness and soil development was beyond the scope of this investigation, and capping loess units were included in the fan units that the loess overlies. However, loess deposits were the target sample material for infrared stimulated luminescence analysis, and we assessed the relative age for these specific loess deposits through field work and LiDAR terrain analysis.

The tributary alluvial fan deposits have distinctly different geomorphic characteristics to the west and east of the entrance to the Lower Yakima River Canyon (Figure 3). Therefore, ensuing description contrasts the west-of-the-canyon and east-of-the-canyon range front. Along the range front east of the canyon entrance, the tributary alluvial fans are thin (1 – 3 m), expansive, dissected and extend up to 2.5 km onto the Kittitas Valley floor. Six generations of increasingly higher and older fans are mapped based on geomorphic preservation and morphostratigraphic position (Figure 6). Field exposures indicate fan surfaces were deposited unconformably onto the Upper Ellensburg Formation (Tue), the unconformity representing the paleo-pediment that bounds the southern margin of Kittitas Valley. Successively younger fans

originate at the mouth of older entrenched fan deposits and extend further northward onto the valley floor. Younger fans also are nested and inset within older fan systems (Figure 6). The scarcity of Yakima River lithofacies within the distal edge of the terraced fan deposits adjacent to the valley floor combined with extensive Quaternary fan progradation of the locally derived sidestream gravel confirms that the Yakima River has not migrated to the east of the canyon entrance during the late Quaternary.

In contrast, in the west-of-the-canyon range front, tributary alluvial fan deposits are small, the fans are steeper, and the fans are confined within tributary canyons incised into the basalt of the range front. Only the youngest fans extend beyond the tributary mouth onto the Kittitas Valley floor. Based on elevation and geomorphic position along the range front, there are four generations of fan surfaces. Fans are constructed by debris flows that are generated in the steep tributary headwaters and then deposited in the lower reaches within the tributary canyon or on the valley floor of the Yakima River floodplain. Subsequently the distal edges of the alluvial fans are eroded by the Yakima River.

Quaternary Geology of West-of-Canyon Range Front

West of the Yakima River canyon entrance, analysis of LiDAR imagery and field mapping yield abundant evidence for active and entrenched alluvial fans within multiple tributary canyons incised into the range front (Figure 7). Spring Canyon (Figure 3) provides the most complete record with four distinct sidestream alluvial fan deposits representing former elevations of the Spring Canyon tributary channel (Figure 7). The youngest Quaternary fan deposit (Qf1) slopes gently between 5° to 10° onto the valley floor. The next youngest Quaternary fan deposit (Qf2) is well preserved and has the largest areal extent (Figure 7). Unit Qf2 is generally 2-3 meters above active tributary channels and has slopes ranging between of 3° to 10°. Quaternary fan deposit three (Qf3) is best preserved at Spring and Benwy Canyons (Figure 7) and consists of a series of relatively flat lying terraces approximately 10 meters above the active channel. The oldest and most distinct alluvial unit along the west-of-canyon range front, Quaternary fan deposit four (Qf4), is approximately 18 meters above the active tributary channel at Spring Canyon. Unit Qf4 ranges in slope between 5° to 20°.

A composite alluvial fan stratigraphic section of Qf4 at the north distal flank of Spring Canyon (Figure 8A) indicates multiple deposits of sidestream alluvium interbedded with loess units of varying thickness. The thickness of alluvial and loess packages varied with distance to the tributary mouth. Generally, deposits proximal to the tributary channel mouths have thicker packages of alluvium while exposures distal to the tributary have thicker deposits of loess (e. g., Figure 8A).

Lateral erosion by the Yakima River is greater in areas with closer proximity to the lower Yakima River Canyon entrance. Because such lateral erosion trims the range front and accelerates downcutting of tributaries flowing perpendicular to the range front, the relatively older fan deposits are less well preserved in tributaries closest to the canyon entrance. Situated at the flanks of Long Tom and Shushuskin canyons are paleo-Yakima River gravels (Qg5) 82 m to 70 m above the valley floor (Figures 6 and 7). The presence of the Cascade-derived lithology in the terrace gravels implies the Yakima River abutted against the paleo-Manastash range front in Qg5 time. Although unit Qg5 is likely younger than the Thorp Gravel (Waitt, 1979), both the mainstream Thorp Gravel and Qg5 gravel are sourced from the Cascade Range.

Quaternary Geology of Yakima Canyon Entrance

A series of strath terraces occur in the Yakima River Canyon two km south of the canyon entrance (Figure 9). The Yakima Canyon terraces are located on the northern and southern edge of an abandoned meander (Figure 9A) and illuminate the history of incision through the Manastash Ridge by the Yakima River. The elevationally higher northern terraces, 40 to 135 m above the meander loop, document the initial creation and subsequent incision of the meander. Paleo-Yakima River gravels (units Qg6, Qg5, and Qg4) exposed within the tributary canyons and southern flanks of the terraces are unconformably deposited on Columbia River Basalt (Figure 9). These paleo-Yakima River gravel units are in turn overlain by tributary fan alluvium (units Qf5, Qf4) (Qg4 overlain by Qf4, Figure 8B). The distinct contrast of mainstream river gravels (Qg5, Qg4) overlain by sidestream lithofacies (Qf5, Qf4, Qf3) within the terrace sequence suggests abandonment by the Yakima River was followed by fan building.

In contrast, the southern terrace sequence (Qg2 overlain by Ql2), south of the abandoned meander loop, is younger and lower in elevation than units Qg5 and Qg4 and documents incision post-abandonment (Figure 9). Terrace exposures record a bedrock strath surface cut on Columbia River basalt 19-20 m above the Yakima River channel. The strath is overlain by a 6 to 7 m thick paleo-Yakima River gravel package (Qg2), which is in turn overlain by a 3 m thick clean loess (Ql2) (Figure 8C).

Age Determinations for Quaternary Units

Infrared stimulated luminescence (IRSL) age determinations were performed by Shannon Mahan at the USGS Luminescence Dating Lab, Denver, CO on silt and fine sand samples from fan and terrace deposits west of the canyon mouth and within the canyon (Table 1). Quartz optically stimulated luminescence (OSL) was initially planned, but because of a slow decay signal retrieved from the samples during luminescence, quartz OSL was abandoned. An alternative approach, Infrared Stimulated Luminescence (IRSL), involves luminescence of K-feldspars using infrared diodes. For younger samples (< 100 ky), IRSL dating works well. For older samples (> 100 ky), IRSL ages are too young, which is a function of "anomalous fading" of K-feldspars (Morthekai et al., 2011). Anomalous fading is an observation where electrons "tunnel" from principal luminescence traps to nearby structural defects in sediment. Anomalous fading of the feldspars from infrared stimulated luminescence analyses produced an underestimate of ages for several samples (MN10-1, MN10-3, MN10-4, and AM10-2). For these samples, a fade correction was used (13% fade rate, after Morthekai et al., 2011) to determine minimum ages of the sample (Table 1). Three loess exposures intercalated within Qf4 sidestream alluvial deposits along the west-of-the-canyon range front (MN10-1, MN10-3, MN10-4) produced fade-corrected IRSL minimum ages ranging between 215,880 ± 10,310 and 279,020 ± 31,240 (Table 1).

Analysis of a loess (MN10-5) capping Qf3 in the west-of-canyon range front area indicated an IRSL age of 20,860 ± 1,520 (Table 1, Figure 7). Based on the large difference between IRSL ages of Qf3 (20.9 ka) and Qf4 (>280 ka) and between a tephrachronologic age for Qf3 (100 ka; see below) versus the IRSL age for loess capping Qf3 (20.9 ka), we conclude that the loess cap of Qf3 (sample MN10-5) represents deposition that is an order of magnitude younger than the underlying alluvial deposit Qf3. Therefore the IRSL sample MN 10-5 does not inform the age of Qf3.The alternative 100 ka age for Qf3, discussed below, comes from tephrachronology.

Infrared stimulated luminescence (IRSL) analyses were also performed for the mainstream paleo-Yakima River alluvial deposits or overlying loess situated within or adjacent to the abandoned meander loop near the lower Yakima River Canyon entrance (Figure 9). IRSL samples were acquired from the northern (Qg4) and southern (Ql2) strath terrace sequences (samples AM10-2 and AM10-1 respectively, Figures 8B and 8C). The Qg4 terrace sediment produced a minimum age of 254,250 ± 17,080 and the Ql2 loess cover above Qg2 terrace gravel produced an age of 88,750± 4520 (Table 1). Therefore infrared stimulated luminescence analyses indicate the Yakima River was actively incising within the meander at 250 ka and the Yakima River had abandoned the meander loop by 90 ka.

Tephra sample TL100110-1 was collected at the distal edge of fan deposit Qf3 adjacent to the mouth of Spring Canyon (Figure 7). The 5 cm thick discontinuous tephra unit, which was intercalated with fan alluvium, appeared to be a reworked airfall tephra deposit. Based on microprobe investigation of glass in the tephra, the glass correlates well (0.976 and 0.96) to the 100 ka Carp Lake (CL-90A or CARP-10) tephra sequence (Carp Ash-10 of Whitlock et al., 2000) (E. Wan, U. S. G. S. Tephrachronology Laboratory, written communication, March 31, 2011). The Carp Lake tephra is not dated directly but rather is extrapolated from an age-depth regression model for a core from Carp Lake (Whitlock et al., 2000). The younger age bound was determined by thermoluminescence methods on a sample stratigraphically above CARP-10 (Berger and Busacca, 1995), and the older age bound was determined from deeper (older) tephra with distinctive glass geochemistry. Given that the deeper, older tephras (218 and 190 ka) are only 2 m lower in the core than the 100 ka tephra, it is possible that the 100 ka Carp Lake tephra could actually be tens of thousands of years older than 100 ka.

Incision Rates of the Yakima River and Range Front Tributaries

In order to quantify incision within the study area, we calculated incision rates using IRSL age constraints. Two incision rates were determined for the mainstream Yakima River alluvial deposits from the southern and northern terrace sequence within the Yakima Canyon entrance (Figure 8; Table 2). The southern strath terrace stratigraphic sequence (sample AM10-1) yielded an incision rate of 0.16-0.18 m/1000 yr. The IRSL age constrains the age of the capping loess (Ql2) and the strath at the base of the underlying alluvial gravel (Qg2) is 9 m below the sample site in loess (Figure 8C). The actual age of inception of incision into the strath surface would be older, by the amount of time required to deposit 2 m of loess, assuming that the gravel is coeval with the age of strath formation. Therefore the true incision rate may be slightly less.

Fluvial terrace deposit Qg4 from the northern strath terrace sequence (Figures 8 and 9B) yielded incision rates of 0.18 to 0.20 m/1000 yrs (Table 2). However, the age used to calculate the incision rate for the Qg4 terrace (sample AM10-2, Table 1) was based on a fade-corrected IRSL age determination that represent a minimum age; therefore, this age only constrains an upper bound to the incision rate for paleo-Yakima River deposit Qg4.

Range Front Faulting and Fault-Related Deformation

The principle structure of Manastash Ridge is the large, open asymmetrical Manastash anticline and associated range front fault system (Figures 6 and 10). The forelimb of the Manastash anticline is composed of two small subsidiary structures, the Manastash syncline and Thrall anticline (Bentley, 1977) (Figure 10). Along strike to the northwest, northeast-vergent

range front thrust faults daylight; and to the southeast, a range front thrust fault does not daylight but a backthrust is evident in the forelimb of the Manastash anticline.

Two approaches were employed to investigate range front and fault related deformation. The first approach was Quaternary geologic mapping of the range front in conjunction with analysis of LiDAR imagery. The second approach was to investigate deformation in cross section at two transects where structure is revealed across strike perpendicular to the range front. One of the transects is along the Yakima River canyon where roadcut exposures and natural exposures in the steep canyon walls provide insight to deformation and faulting. The other transect is along Shushuskin Canyon, which is incised into the range front. Although the road along the canyon bottom provides some exposures that reveal bedrock structure, the main source of structure and fault data along Shushuskin Canyon is a seismic reflection line shot along the road alignment.

The Manastash range front fault system trends along the base of the range front west of the canyon entrance. As identified using LiDAR, seismic imagery and field mapping (Figures 6 and 11), the range front fault system west of the canyon entrance consists of two distinct thrusts fault systems ('northern fault system' and 'southern fault system') (Figure 7). The northern fault system, trending N40°W north of Shushuskin Canyon and N60°W south of Shushuskin Canyon, delineates the transition from the gently sloping valley floor and Yakima River floodplain to the moderately sloping alluvial deposits at the north margin of the range front. The northern trace of the range front fault system, only mappable west of the canyon entrance, juxtaposes the older upthrown alluvial unit Qf4 with younger and lower alluvial unit Qf2 (Figure 7B). This fault is also seen on the seismic reflection line trending along Shushuskin Canyon. The seismic imagery depicts the fault scarp, 5 m to 15 m high, daylighting at station 470 (Figure 11). The highly reflective, shallow and sub-horizontal alluvial sediments on the northeast side of the inferred fault are thrust under brecciated basalt units that bound the southwest side of the northern range front fault (Figure 7B and 11). The alluvium-basalt contact is noted by the strong reflection between depths of 350 to 400 meters in the footwall of the northern range front fault. The 350-400 m depth of the contact indicates the minimum vertical offset of the range front fault system (Figure 11).

Moving further southeast along the range front, the northern fault system splays at Dead Cow Gulch North into two distinct fault scarps (Figure 7). The lower and younger fault scarp, 5 to 11 m high, juxtaposes alluvial units Qf1 and Qf2 (Figure 7). Based on the steepness of the scarp face, we infer the scarp may be Holocene in age. A small exposure of both Columbia River basalt (Tw) and Ellensburg Formation (Teu) outcrops on the upthrown (southern) side of this fault (Figure 7) and documents uplift along the hanging wall. The upper and older fault scarp at Dead Cow Gulch South, which trends N55°W, is similar to the fault scarp expressed at Long Tom Canyon and juxtaposes units Qf4 and Qf2 (Figures 6 and 7).

Moving even further southeast from Dead Cow Gulch South, the surface traces of northern fault system move out onto the valley floor and any evidence of recent faulting has been removed by Yakima River erosion. Elevated and abandoned alluvial deposits within Spring Canyon and at the mouth of Benwy Canyon are consistent with the presence of northern range front fault extending out onto the valley floor west of the canyon entrance (Figures 6 and 7).

The southern range front fault system traces a paleo range front-valley floor junction that follows the southwestern contact of unit Qf4. Adjacent to Shushuskin and Long Tom Canyons, the southern range front fault scarp, approximately 20 m high, juxtaposes paleo-Yakima River deposit Qg5 to the southwest and unit Qf4 to the northeast (Figure 7). Where the scarp crosses

the seismic line, the seismic line images a fault daylighting at the surface (Figures 6 and 11). Moving southeast of Shushuskin Canyon, the southern range front fault juxtaposes basalt to the southwest with alluvial unit Qf4 to the northeast. Based on subsurface seismic imagery, we infer that the southern range front fault daylights at station 260 on the seismic line (Figure 11) and truncates both a syncline in the hanging wall and an anticline in the footwall. Therefore, the anticline-syncline sequence that is better exposed along the Yakima Canyon road is also evident at Shushuskin Canyon where the syncline–anticline sequence has been thrust over itself along southern range front fault (Figure 11).

We infer that the distinct topographic break-in-slope, evident along the range front between Long Tom Canyon to the northwest and Shushuskin Canyon to the southeast (Figure 7A) and traced by the contact between basalt and alluvial unit Qg5 (Figure 7B), is due to fluvial incision as the Yakima River abutted against the basalt range front. The presence of paleo-Yakima River deposits Qg5 is consistent with incision and trimming of the range front by the Yakima River followed by uplift and isolation of alluvial deposits Qg5 and Qf4 due to slip on the southern range front fault system.

The other fault associated with the Manastash range front fault system is a backthrust; this backthrust is the only surface expression of faulting within, and east of, the canyon entrance. Deformation 0.6-1.2 km south of the Manastash range front is well exposed in road cuts in the Yakima River canyon south of the canyon entrance. Bentley (1977) discusses deformation inferred from these exposures. Stratigraphy of individually identified basalt and interbasalt units evident in the canyon road exposures (Bentley, 1977), in conjunction with bedding attitudes, documents the folded structure of the Manastash anticline forelimb (Figure 10A). We supplemented Bentley's (1977) lithologic mapping with strike and dip measurements along the road cuts and infer that a steeply dipping backthrust intersects the Manastash Syncline axis to accommodate the truncation of the Squaw Creek Member (Tesc) in the northern limb. The disappearance of the Squaw Creek Member on the northern limb is a consequence of uplift and erosion of the hanging wall of the backthrust (Figure 10A). Based on the structural trend of bedrock exposures 0.75 km south of the canyon entrance, we infer that the steeply dipping backthrust trends N60°W. Striations and slickenlines noted within the Manastash syncline yield a predominate trend sub-perpendicular to the fold axis suggesting shearing was primarily due to flexure as the syncline tightened. Trend and plunge observations indicate primary dip-slip motion because striation and slickenline rakes range from 41° to 65°.

In summary, a combination of field mapping and interpreted fault geometry from seismic imagery indicates the range front fault system west of the canyon entrance consists of two reverse faults that dip approximately 30° south under Manastash Ridge (Figures 7 and 11). These two reverse faults do not extend as subaerially discernable traces eastward into the canyon entrance area. Rather, a backthrust in the deformed forelimb of the Manastash anticline characterizes the faulting in the canyon entrance area. Road cut exposures at Vanderbilt Gap 5.2 km to the east-southeast show a steeply dipping backthrust truncating the southern limb of a syncline (Bentley, 1977), from which we infer that the backthrust evident in the Yakima River canyon exposures continues eastward along strike to Vanderbilt Gap.

Longitudinal Stream Profiles and Tributary Knickpoints

Eight tributaries (Northeast 1, Northeast 6, Noname Canyon, Benwy Canyon, Spring Canyon, Dead Cow South, Dead Cow North and Shushuskin Canyon; Figure 3) were chosen to investigate channel longitudinal profiles across the range front and determine respective tributary

concavity (θ). Because rate of fluvial incision responds to the rate of baselevel fall, a graded river profile demonstrates fluvial equilibrium (Zaprowski et al., 2005). Yet bedrock rivers, because of the inability of bedrock channels to quickly adjust to external perturbations, tend to retain evidence of disequilibrium due to tectonic, climatic, and/or eustatic driving mechanisms. Knickpoints within the longitudinal profile, and concavity (θ) values, can provide a proxy for areas along the range front where the fluvial systems are in disequilibrium due to climatic and/or tectonic influences (Kirby et al, 2001, Snyder et al., 2000, Wobus et al., 2006).

Two tributaries, Northeast 1 and Northeast 6, were chosen from east-of-the-canyon range front for profile and knickpoint assessment (dashed profiles, Figure 12A). Based on the lack of evidence of range front faulting, we infer the tributary channels should not be perturbed by baselevel fall. Concavity (θ) values of the two tributaries range between 0.44 and 0.60 (Northeast 1 and Northeast 6, Figure 13). These values are consistent with a profile that has a moderately steep concave headwater profile followed by a gentle, smooth sloping profile grading to the valley floor (Figure 12). Lack of knickpoints within these longitudinal profiles as well as the range of concavity values corroborate our inference that these tributaries from the east-of-the-canyon range front have experienced minimal fluctuation in baselevel.

In contrast, six tributaries were analyzed from west-of-the-canyon range front that flow perpendicular to the range front fault system. The tributaries demonstrated irregular headwater profiles followed by steeply sloping channel geometries with concavity (θ) values that range between 0.11 to 0.48 (Figures 12 and 13). Tributaries Noname, Benwy and Spring canyons all exhibited a knickpoint along the lower reach of their respective channel profile at a correlative elevation of approximately 510 meters (Figure 12B).

Knickpoints responding to the same baselevel change tend to be found at constant elevation among tributaries systems of different drainage area because knickpoints migrate through fluvial systems at a rate proportional to tributary drainage area (Wobus et al., 2006). A coincident knickpoint across the three adjacent tributary channels indicates a migrating wave of incision responding to same event of baselevel lowering.

To understand how knickpoints relate to the entrenched alluvial fans, we superimposed the entrenched alluvial fan surface elevations onto the longitudinal profile of Spring Canyon (Figure 14). Point elevations from each alluvial unit (Qf2, Qf3, Qf4) were projected horizontally onto the vertical plane containing the channel thalweg thereby defining fan surface elevations above the tributary thalweg. If we project a relict channel profile of Spring Canyon downstream from the knickpoint at 510 m, such a relict profile would intersect the surface elevations of alluvial fan unit Qf4 (Figure 14B). Therefore, unit Qf4 records a paleo-channel elevation prior to baselevel fall (Figure 14). The knickpoint on the profile at 510 m elevation records the present position of the knickpoint that started to retreat headward upon initiation of baselevel fall at the time that Qf4 was active. By inference, each successively lower entrenched alluvial unit indicates a separate baselevel lowering event accommodated by incremental lowering of the Kittitas Valley floor relative to the mouth of Spring Canyon.

DISCUSSION

Base-level Lowering Mechanisms

Based on tributary longitudinal profiles, knickpoints in profiles and fault scarps at range front positions, we infer periodic episodes of baselevel fall within the tributaries draining northward off the Manastash range front onto the Yakima River flood plain. Two candidate mechanisms driving episodic baselevel fall are tectonic uplift of Manastash Ridge or erosional

lowering of the Yakima River floodplain and the Kittitas Valley. In a tectonic model, we predict uplift of the range front concurrent with genesis of fault scarps, while a climatic model would require progradation of fans onto the Kittitas Valley floor followed by erosion of fans and erosional lowering of the Kittitas Valley by the Yakima River. Conceptually, either mechanism can produce entrenched alluvial fans, range-front scarps, and induce a migrating knickpoint response within tributary systems (Schumm, 1993; Ritter et al., 1995). The subsequent discussion will evaluate each mechanism in relation to observations within the study area.

A tectonic model is consistent with the regional tectonic context of the Yakima Fold Belt (Riedel et al., 1993, Price et al., 1989); and in applying the structural context locally, we would infer that the steeply dipping Manastash anticline forelimb is folded and uplifted by a north verging thrust fault daylighting within the Manastash range front. Periodic uplift along the hanging wall of a south dipping thrust fault would accommodate growth of the Manastash anticline, generate range front fault scarps, and lower the valley floor baselevel. In contrast, the competing driving mechanism of baselevel lowering would be erosional lowering of the Kittitas Valley by the Yakima River.

Glaciation in the Upper Yakima River Canyon and Northern Kittitas Valley

Mapping of six distinct Pleistocene glacial outwash terraces document alpine glacier advances into the northern Kittitas Valley and subsequent aggradation (Porter, 1976). Sequences of outwash terraces, 5 m to 140 m above the active Yakima River channel, indicate periods of aggradation followed by fluvial degradation and incision. Porter (1976) used pedogenic and weathering rind analyses to divide the alpine glacial sequence in the northern Yakima River Canyon into two major glacial advances that are recorded by the Kittitas Drift and the Lakedale Drift. The Kittitas Drift corresponds to the penultimate glacial advance (marine isotope stage 6), which peaked between 130 to 140 ka, and is composed of two glacial phases, the Swauk Prairie member and Indian John member (Porter, 1976; Waitt, 1979). Outwash terraces adjacent to terminal moraines from the Kittitas Drift are situated 100 m above the Yakima River exposing extensive fluvial boulder-cobble units intercalated with finer pebble/sand units (Porter, 1976). The Lakedale Drift is composed of several outwash terraces, 5 to 10 m above the Yakima River channel, and correlates to the Frasier Glaciation of the Puget lowland that reached maximum extent 14,000 yr ago (Waitt, 1979).

In summary, the Yakima River and Kittitas Valley have experienced dramatic shifts in sediment yield and transport capacity due to late Quaternary climate fluctuations. The presence of glacial outwash terraces extending into the Kittitas Valley is evidence for climatic fluctuations that fostered cycles of aggradation (transport-limited conditions) and incision (supply-limited conditions). A terminal moraine impounded sediment and meltwater during retreat of the Indian John glacial phase creating a lake 275 m deep, 15 km long and 3 to 5 km wide. When breached, the lake must have caused massive aggradation and erosion in the Kittitas Valley (Porter, 1976).

Climatic Forcing along the Manastash Range Front

While tectonics generates relief, alternating fan building and entrenchment within active tectonic environments are related principally to climate (Ritter et al., 1995; Spelz et al., 2008). In an alluvial fan model for arid environments proposed by Bull (1991), periods of fan building coincide with transition from glacial to interglacial cycles where warming conditions and lack of soil moisture and vegetation cover yields an increase in sediment production causing aggradation and fan building. Aggradation continues until a geomorphic threshold is crossed wherein the

hillslope sediment reservoir is depleted, and the fluvial system becomes supply limited. Sediment supply-limited conditions initiate incision and entrenchment (Bull, 1991; Spelz et al., 2008). In an alternative model for fan building, Harvey et al. (1999) infer that inset alluvial fan sequences are associated with wetter conditions associated with glacial periods. Fan building would be synchronous with deposition of outwash terraces. As the climate conditions altered to interglacial periods, incision and entrenchment would dominate the geomorphic system (Harvey et al., 1999). Regardless, a diagnostic attribute for climate forcing is synchronous aggradation followed by synchronous incision within a region (Ritter et al., 1995).

Porter (1976) and Waitt (1979) document glaciation and subsequent aggradation in the Upper Yakima River Valley and the upper Kittitas Valley, but it is unclear if the Manastash range front and Lower Yakima River Canyon were similarly affected by aggradation during glacial periods. However, ages of alluvial deposits along the Manastash range front can constrain timing of fan aggradation. IRSL analysis of a capping loess deposit (Ql2) within the canyon entrance indicates that 2-m thick loess is 90 ky in age and that the aggradation of Qg2 is thus slightly older than 90 ky (Table 1), while based on tephrachronology we infer that Qf3 was actively prograding at 100 ka or even tens of ky prior to 100 ka. Therefore, aggradational timing of Qf3 and Qf2 appears to be post-Kittitas Glaciation (130-140 ka) and well before Lakedale glaciation (14 ka). Based on the above age estimates, we infer that aggradation of Qf3 and Qf2 is associated with the oxygen isotope stage 5 interglacial, which was the interglacial period directly following the Kittitas Glaciation in the time period from approximately 130 ka to 100 ka. Aggradation during interglacial dryer and warmer conditions favors a fan-building model consistent with the arid model proposed by Bull (1991). IRSL analyses for Qf4 consistently yielded a minimum age to be 250 ky (Table 1), which suggests aggradation of Qf4 predates the Kittitas glaciation (predates 140 ka). A minimum age constraint does not permit correlating aggradation of Qf4 to a specific glacial and interglacial cycle. However, geomorphic mapping of fan deposits along the entire range front predicts a cyclic pattern including up to three periods of fan building older than Qf4 (Figure 6). The widespread distribution of fans of varying relative ages, between the east-of-canyon range front and Yakima River Canyon mouth, indicates that the primary driver for fan aggradation is uniform climatic conditions affecting the entire range front.

Alluvial fans along the west-of-canyon range front are distinctly separated by scarps ranging in height from 5-20 m (Figure 7). If we assume climate is the driver of fan aggradation episodes, what process is accountable for the distinct separation of fans by scarps? Porter (1976) documented periods of aggradation within the Kittitas Valley, causing a temporary increase in baselevel, which was then followed by entrenchment, incision and baselevel lowering. However, preservation of an erosional scarp along the range front that truncates the distal edge of fans requires, first, fan progradation onto the Kittitas Valley floor and, second, migration of the Yakima River laterally southwestward thereby eroding the distal edges of the alluvial fans and creating an erosional escarpment. At Dead Cow Gulch South for example, Qf2 would have been deposited during aggradation of the fan onto the Kittitas Valley followed by southwest migration of the Yakima River towards the range front so that an erosional scarp could be developed on the Dead Cow Gulch South fan. The higher elevation scarp that extends from Long Tom Canyon southeastward across Shushuskin Canyon (Figure 7A) could be explained with the same mechanism, but during a previous aggradation and degradation cycle. However, for the scarp to be higher and elevationally separated from the Dead Cow scarp, the entire Kittitas valley would have had to have been lowered erosionally between times of Long Tom Canyon fan building and times of Dead Cow South fan building because the Long Tom canyon scarps are 24-36 m higher

than the Dead Cow South scarps. While it is plausible for the two sets of scarps to be generated exclusively by climatically-driven cycles of deposition and erosion, it would be unlikely because lowering the entire Kittitas Valley by up to 35 m in about 200 ky (approximate age difference of of Qf4 and Qf2) requires a valley-wide incision rate of about 0.18 m/ky. We infer that, based on the elevational difference between the two sets of scarps, the conspicuous alignment evident within each scarp set, and the observation that the two scarp sets juxtapose alluvial units of different ages (Figure 7), these scarps are fault scarps not erosional features.

Other criterion for evaluating the role of climate forcing in generating baselevel fall along the Manastash range front are tributary longitudinal profile form and profile concavity (θ). There are differences in channel geometry, concavity (θ) values and presence or absence of knickpoints in east-of-canyon tributaries compared to west-of-canyon tributaries. By inference, the two fluvial systems are differentially influenced by tectonic forcing (Kirby et al, 2003). Irregularities in channel geometry that can be attributed to tectonically induced baselevel fall are only found within the west-of-the-canyon range front tributaries where a range front fault system is identified. Conversely, a climate signal is most prominent within east-of-the-canyon fluvial system where there is no evidence for tectonic forcing. By using the distinctions of concavity values and presence or absence of knickpoints between the two fluvial systems, we can decouple the climatic and tectonic signals.

High concavity values, as noted within east-of-the-range front tributaries (θ = 0.44 and 0.60), suggest that uplift rates decrease in the downstream tributary direction (Kirby et al., 2001). Geologic mapping (Figure 6) corroborates that the east-of-canyon range front exhibits no surficial evidence of fault scarps and that the high relief and commensurately more tectonic uplift likely is confined to the ridgeline to the south. Furthermore, cyclic entrenchment of older alluvial fans followed by deposition of younger fans prograding outward onto the valley floor ultimately producing a large broad nested alluvial fan is indicative of a climate signal (Bull, 1991; Ritter et al., 1995 and Spelz et al., 2008). Inset fans document that incremental fan growth basinward was accommodated by entrenchment and dissection of older fan units by the steep, small, ephemeral tributaries flowing northward onto the valley floor. Lack of any channel knickpoints within the east-of-canyon tributaries (Figure 12) suggest profile equilibrium, where the rate of incision is balanced with baselevel lowering. These small tributaries with weak erosive ability demonstrate channel profile equilibrium and suggest a low magnitude baselevel lowering signal congruent with a fluvial system driven by gradually changing climatic conditions.

Paleo-range front elevations along the east-of-canyon range front are represented by upper Ellensburg Formation (Teu) exposures that underlie the alluvial fan deposits. The paleo range front elevations are elevationally similar to the contact of Teu and overlying Thorp gravel on the erosional remnant of Potato Hill 1.5 km to the north (Figure 3). Based on a cross section that connects the paleo-range front and paleo-Kittitas Valley at Potato Hill (Figure 15), the Kittitas Valley floor has been erosionally lowered 26-37 m since deposition of 3.7 Ma Thorp gravel (Waitt, 1979) on top of the Upper Ellensburg Formation (Teu) at Potato Hill.

West-of-the-canyon range front fluvial systems demonstrated a wide variation in concavity values (0.11 to 0.48). The complex longitudinal profile geometry of Spring Canyon made determining the concavity difficult to assess (Figure 14). The large convexity within the headwater of Spring Canyon was attributed to colluvial-dominated processes causing the limits for determining the concavity to be extended downstream of the prominent convexity (Figure 14). Concavity values calculated for tributaries Noname, Benwy and Shushuskin exhibited low values ranging between 0.11 to 0.38 (Figure 13). Low concavity values in tectonically active

areas have been noted in fluvial systems where the uplift rate increases downstream (Kirby et al., 2001). Here we infer that uplift rate increases downstream within the west-of-the-canyon range front tributaries as a consequence of the range front fault system. In addition, an elevation-coincident knickpoint, noted among the Noname, Benwy, and Spring Canyon tributaries, suggests the fluvial systems are responding to a synchronous baselevel fall among these tributaries (Wobus et al., 2006). Documentation of disequilibrium through coincident knickpoints among channel profiles and low concavity values for the west-of-the-canyon tributaries, and the apparent channel profile equilibrium within the east-of-the-canyon tributaries, is consistent with the inference that tectonic motion dominates landscape evolution west of the canyon entrance.

Range Front Fault System

Distinct southwest-side-up fault scarps, at the mouth of Long Tom Canyon and at the mouth of Dead Cow Gulch South, collectively delineate the northern range front fault system (Figure 7). There are two fault scarps adjacent to the mouth of Dead Cow Gulch South because a younger fault stand, which juxtaposes Qf1 and Qg2, splays off the older fault strand that juxtaposes Qf2 and Qf4. Therefore, younger faulting propagates northward as the fault splays to lower topographic levels (Figure 7).

The presence of the southern range front fault scarp is inferred from geomorphology, geologic mapping and from seismic reflection data. Interpreted geometry of the southern range front fault from seismic imagery depicts a shallow (~20°) south dipping fault. The shallow dip of the fault system is corroborated by the sinuous nature of the mapped fault trace (Figure 7). Furthermore, the diffuse nature of the southern range front fault line scarp suggests little contemporary fault activity during the late Quaternary because motion transferred onto the northern range front fault system. The presence of three distinct south-to-north fault lineaments, southern range front fault, southern strand of northern range front fault and the shorter northern strand of the northern range front fault, collectively documents progressive northward advancement of range front fault system where the southern fault offsets relatively older Quaternary units while the northern most fault offsets the youngest alluvial fan unit. All three north-vergent range front faults trend across the Dead Cow Gulch South tributary (Figure 7).

No distinct fault scarp lineaments were delineated within east-of-the-canyon range front or canyon entrance through field mapping and LiDAR analysis. Based on the lack of evidence for faulting within the east-of-the-canyon range front, we infer that the north vergent faulting, apparent at the surface west of the canyon, becomes blind (i. e., does not daylight onto the land surface) going along strike to the southeast. However, a south-vergent backthrust at higher structural levels is inferred from structural and stratigraphic observations within the canyon entrance (Figures 8 and 10). This backthrust fault trends southeast on and just south of the Manastash ridgeline and is probably the same as the southwest-side-up thrust fault mapped by Bentley (1977) at Vanderbilt Gap 7 km along strike to the east-southeast.

The difference in deformation style between east-of-the-canyon range front where the master reverse fault is blind and west-of-the-canyon range front where the master reverse fault reaches the surface is exemplified by the contrasting geomorphic expression of Manastash Ridge. Manastash Ridge adjacent to east-of-the-canyon range front is punctuated and has an ‘en echelon’ pattern along the ridgeline consistent with inferred surface faulting associated with the steeply dipping backthrust. In contrast, Manastash Ridge adjacent to the west-of-the-canyon is a

broad, flat topographic highland, which is inferred to be related to north verging, ramp-fault geometry (Figure 10).

There are two lines of evidence that the master reverse fault evident west of the canyon continues, possibly as a blind structure, along strike to the southeast across the canyon entrance. First, assuming that incision rates are equivalent to uplift rates within the anticline, strath terraces in the canyon have uplift rates on the order of 0.16 - 0.20 m/ky (Table 2) based on incision rates of the Qg2 and Qg4 strath terrace sequences. The uplift of the hanging-wall is a consequence of slip on the south dipping ramp master thrust (Figures 8 and 10). Second, in the canyon entrance area there is geomorphic and seismic-reflection-data evidence for a north-vergent fault that strikes southeast. A seismic reflection line collected early in 2012 along the road that follows the canyon floor in the canyon entrance area shows such a structure (communication from T. Pratt, August 2012), and this structure is on trend to the southeast with a northeast-facing slope inflection in the range front that is a candidate fault scarp based on analysis of the LiDAR imagery.

Comparative incision rates, hanging wall versus footwall, Manastash range front fault system

As summarized above, the incision rate within the hanging wall of the Manastash fault system, 0.16-0.18 and 0.18-0.20 m/ky (Table 2), is represented by the incision rates for the Qg2 and Qg4 strath terraces within the Yakima River abandoned meander.

The incision rate on the footwall of the Manastash range front fault is represented by the lowering the of the Kittitas Valley relative to the isolated, elevated remnant of the paleo-valley floor at Potato Hill (Figures 3 and 15). The paleo valley floor at Potato Hill is the Ellensburg/Thorp contact and is 26-40 m higher than the modern valley floor. Using an age for the Thorp gravel of 3.7 My (Waitt, 1979), the lowering rate of the Kittitas Valley floor is 0.01-0.007 m/ky. Therefore the incision rate of the hanging wall is more than an order of magnitude more than the incision rate of the footwall, and the incision rate difference is about 0.15-0.19 m/ky. Again, assuming that within the anticline incision rates are equivalent to uplift rates, then we infer that the uplift rate of the Manastash ridge relative to the valley floor is on the order of 0.17 m/ky over the last 4 My (assuming that the uplift rate of the last 90 ky may be projected back in time at least until 3.7 Ma). Based on the fault scarps ranging from 5 to 20 m high within the northern range front fault system, the fault scarps must represent multiple earthquake events; and it is the resulting tectonic uplift as a consequence of such earthquakes that, over several millennia in the Quaternary, has constructed the Manastash range front and Manastash Ridge at the southern end of the Kittitas Valley.

CONCLUSIONS

We designed data collection and data analysis to address hypotheses that the Manastash anticline is an actively growing fold, that thrust faulting is the driving mechanism for folding, and that thrust faults daylight at the range front. Two fault scarps at the base of the Manastash range front each correlate to thrust faults evident on a seismic reflection line across the range front. The northernmost fault scarp cuts the youngest alluvial fan; and from the youthful appearance of the scarp, the last earthquake that freshened the scarp may be Holocene in age. Based on projection downward of the thrust faults evident on the seismic line, we infer these faults root in a master ramp thrust. Because the faults that daylight at the surface have been active in the Quaternary, we infer the Manastash anticline is an active growing fold above a master ramp thrust. Support for the inference that the Manastash anticline is an actively growing

fold are uplift rates determined along the Yakima River within the core of the anticline; these contemporary uplift rates, spanning the last 90 ky, are 0.16-0.18 m/ky.

Steep and short tributaries draining off of Manastash Ridge deposit fans at the range front along the southern edge of the Kittitas Valley; and where active faulting occurs at the base of the range front, the fans are progressively truncated and uplifted by ongoing Quaternary faulting. Because fan growth is episodic and most vigorous during periods following alpine glacial maxima in the Cascade Mountains to the west, discrete packages of fan-deposited debris become geomorphically separated by elevation. This separation by elevation is the product of persistent range front displacement (up to the south) occurring concurrently with episodic fan deposition. Periods with little or no fan building are times when previously deposited fans are elevationally isolated from the base of the range front by thrust faulting. The uplift engendered by the thrust faulting lowers base level for tributaries draining to the Kittitas Valley. Knickpoints in these tributaries, at equal elevation across several tributaries, attest that base level fall affects all tributaries similarly and that the base level fall is the product of co-seismic tectonic uplift events (earthquakes) on the range front.

ACKNOWLEDGMENTS

Brian Sherrod of the U. S. Geological Survey (USGS) provided input in all phases of this project and arranged for the use of the Army Corps of Engineers LiDAR data. Tom Pratt (USGS) shared with us the seismic line data collected through Shushuskin Canyon and discussed with us seismic line data collected through the lower Yakima River canyon at the upstream (northern) canyon entrance. Elizabeth Barnett (USGS) contributed the base data for Figure 2. Elmira Wan (USGS Tephrachronology Laboratory, Menlo Park) performed micro probe analyses of glass samples to determine tephra correlation ages. Shannon Mahan, (USGS Luminescence Dating Lab, Denver) performed luminescence analyses for samples of loess and alluvium from the Manastash range front area. We thank numerous landowners along the Manastash range front for granting access to their lands in order to map geology and collect samples. Landowners Rob and Louise Acheson were especially accommodating.

REFERENCES

Bentley, R. D., 1977, Stratigraphy of the Yakima basalts and structural evolution of the Yakima ridges in the western Columbia Plateau, in Brown, E.H. and Ellis, R.C., editors, Geological Excursions in the Pacific Northwest: Western Washington University, p. 339-390. Published as a geology field guide in conjunction with the 1977 annual meeting of the Geological Society of America.

Berger, G. W. and Busacca, A. J., 1995. Thermoluminescence dating of late Pleistocene loess and tephra from eastern Washington and southern Oregon and implications for the eruptive history of Mount St. Helens: Journal of Geophysical Research, v. 100, p. 22361–22374.

Blakely, R. J., Sherrod, B. L., Weaver, C. S., Wells, R. E., Rohay, A. C., Barnett, E. A., and Knepprath, N. E., 2011, Connecting the Yakima fold and thrust belt to active faults in the Puget Lowland, Washington: Journal of Geophysical Research, v. 116, B07105, 33 p.

Bull, W. B., 1991, Geomorphic responses to climatic change: Oxford University Press, 326 p., ISBN 0-19-505570-5.

Campbell, P. C. and Bentley, R. D., 1981, Late Quaternary Deformation of the Toppenish Ridge Uplift in south-central Washington: Geology, v. 9, p. 519-524.

Harvey, A. M., Wigand, P. E. and Wells, S. G., 1999, Response of alluvial fan systems to the late Pleistocene to Holocene transition: Contrasts between the margins of pluvial lakes Lahontan and Mojave, Nevada and California, USA: Catena, v. 36, p. 255-281.

Kirby, E. and Whipple, K., 2001, Quantifying differential rock-uplift rates via stream profile analysis: Geology, v. 29, p. 415-418.

Morthekai, P., Jain, M., Cunha, P. P., Azevedo, J. M., and Singhvi, A. S., 2011, An attempt to correct for fading in million year old basaltic rocks: Geochronometrica, v. 38(3), p. 223-230.

Porter, S. C., 1976, Pleistocene glaciation in the southern part of the North Cascade Range: Washington, Geological Society of America Bulletin, v. 87, p. 61-75

Price, E. H. and Watkinson, A J., 1989, Structural geometry and strain distribution within eastern Umtanum fold ridge, south-central Washington, in Reidel, S. P., and Hooper, P. R., editors, Volcanism and Tectonism in the Columbia River flood-basalt province: Geological Society of America Special Paper 239, p. 265-281.

Reidel, S.P., 1984, The Saddle Mountains: The Evolution of an Anticline in the Yakima Fold Belt: American Journal of Science, v. 284, p. 942-978.

Reidel, S. P. Campbell, N. P., Fecht, K. R., and Lindsey, K. A., 1994, Late Cenozoic structure and stratigraphy of south-central Washington, in Lasmanis, R. and Cheney, E.S., conveners, Regional Geology of Washington State: Washington Division of Geology and Earth Resources Bulletin 80, 159-180.

Ritter, D. F., Kochel, R. C., and Miller, J. R., 1995, Process Geomorphology 3rd Ed.: W.C. Brown Publishers, Dubuque, IA, 539 p.

Schumm, S. A., 1993, River response to baselevel change: implications for sequence stratigraphy: Journal of Geology, v. 101, p. 279-294.

Smith, G. A., 1998, Neogene synvolcanic and syntectonic sedimentation in central Washington: Geological Society of America Bulletin, v. 100, p. 1479-1492.

Snyder, N.P., Whipple, K.X., Tucker, G.E. and Merritts, D.J., 2000, Landscape response to tectonic forcing: Digital elevation model analysis of stream profiles in the Mendocino triple junction region, northern California: Geological Society of America Bulletin, v. 112, p. 1250-1263.

Spelz, R. M., Fletcher, J. M., Owen, L. A., and Caffee, M. W., 2008, Quaternary alluvial-fan development, climate and morphologic dating of fault scarps in Laguna Salada, Baja California, Mexico: Geomorphology, v. 102, p. 578–594, doi: 10.1016/j.geomorph.2008.06.001.

Sweeney, M. R., Busacca, A. J., Gaylord, D. R., 2005, Topographic and climatic influences on accelerated loess accumulation since the last glacial maximum in the Palouse, Pacific Northwest: USA; Quaternary Research v. 63, p. 261-273.

Tolan, T. L., Martin, B.S., Reidel, S. P., Anderson, J. L., Lindsey, K. A., Burt, W., 2009, An introduction to the stratigraphy, structural geology, and hydrology of the Columbia River Flood-Basalt Province: a primer for the GSA Columbia River Basalt Group field trips; Volcanoes to Vineyards, Geologic Field Trips through the Dynamic Landscape of the Pacific Northwest: Geological Society of America Field Guide 15, p.599-643.

Waitt, R. B., 1979, Late Cenozoic deposits, landforms, stratigraphy and tectonism in Kittitas Valley, Washington: U. S. Geological Survey Professional Paper 1127, 18 p.

Washington Department of Natural Resources (1978), Washington geologic maps, 1:100,000 scale, Yakima sheet: http://www.dnr.wa.gov/Publications/ger_geologic_maps_wa.pdf

Wells, R. E., Weaver, C. S. and Blakely, R. J., 1998. Forearc migration in Cascadia and its neotectonic significance: Geology, v. 26, p. 759-762.

West, M. W., Ashland, F. X., Busacca, A .J., Berger, G. W., Shaffer, M. E., 1996, Late Quaternary Deformation, Saddle Mountain Anticline, south-central Washington: Geology, v. 24, p. 1123-1126.

Whipple, K. X, Wobus, C., Crosby, B., Kirby, E. and Sheelan, D., 2007, New Tools for Quantitative Geomorphology: Extraction and Interpretation of Stream Profiles from Digital Topographic Data; Geological Society of America Annual Meeting Course Notes.

Whitlock, C., Sarna-Wojcicki, A. M., Bartlein, P. and Nickmann. R. J., 2000, Environmental history and tephrostratigraphy at Carp Lake, southwestern Columbia Basin, Washington, USA: Palaeogeography, Palaeoclimatology, Palaeoecology v. 155, p. 7-29

Wobus, C., Whipple, K.X., Kirby, E., Snyder, N., Johnson, J., Crosby B., Sheehan, D., 2006, Tectonics from topography: Procedures, promise, and pitfalls: Geological Society of America Special Paper 398, p. 55-74

Wobus, C., Crosby, B., Kirby, E., Sheehan, D., Whipple, K., Synder, N., Ouimet, W., Gasparini, N., Dibase, R., 2008, GSA Short Course: Tectonic Geomorphology

Zaprowski, B. J., Pazzaglia, F.J. and Evenson, E.B., 2005, Climatic influences on profile concavity and river incision: Journal of Geophysical Research, v. 110, F03004, doi:10.1029/2004JF000138.

PUBLICATIONS RESULTING FROM THE WORK PERFORMED

Ladinsky, T. C., Kelsey, H. M., Sherrod, B. L. and Pratt, T. L., 2010, Range-front deformation on the northern limb of the Manastash anticline, Yakima Fold belt, Washington, EOS Trans., AGU, EP53B-0620.

Ladinsky, T. C., Kelsey, H. M., Sherrod, B. L., Mahan, S., Pratt, T. L., and Blakely, R. J., 2012, Tectonic and climatic influences on the deposition and preservation of Quaternary units along the range-front of the Manastash Anticline, Yakima Fold Belt, Washington: EOS Trans., AGU, in press, (December 2012 AGU meeting).

Table 1. Infra-red stimulated luminescence (IRSL) K-feldspar ages, Manastash anticline, Washington (analyses by Shannon Mahan, USGS, Denver, CO)

Location	Elevation (m)	Geologic unit	Sample identification number	Equivalent dose (Gy)	IRSL age (yrs) Fade corrected*
Yakima Canyon	450	Ql2 loess**	AM10-1	235 ± 10.6	88,750 ±4,520
Yakima Canyon	484	Qg4 fluvial gravel	AM 10-2	102 ±5.54	45,000±2,900 254,250 ± 17080*
Shushuskin fan (trailer site)	495	Qf4 fan gravel	MN10-1	108 ± 11.3	47,890 ± 5,340 279,020 ± 31,240*
Dead Cow Gulch	494	Qf4 fan gravel	MN10-3	93.7 ± 3.94	41,810 ± 2,140 228,220 ±11,900*
Dead Cow Gulch	494	Qf4 fan gravel	MN10-4	94.3 ± 3.03	40,240 ± 1880 215,880 ± 10,310*

*Assumes an anomalous fade rate of 13% (13% fade rate after Morthekai et al., 2011). Anomalous fading of K-feldspars: an observation that the field saturation luminescence intensity is less than the laboratory saturation intensity because of electron "tunneling" from principal luminescence traps to nearby structural defects in sediment in field situations.

** Ql2 loess overlies Qg2 alluvium - see Figure 8.

Table 2. Incision rates using uplifted strath terraces, Lower Yakima River canyon entrance, Manastash anticline

Quaternary geologic unit	Site number*	Surface elevation (m)	Elevation of strath (m)	Elevation, modern thalweg (m)	Amount of incision (m)	Sample age, IRSL** (ky)	Incision rate (m/ky)
Ql2	AM10-1	448	442	427	15	84.2-93.3	0.16-0.18***
Qg4	AM10-2	478	476	428	48	237-271	0.18-0.20****

* See Table 1.

** Fade corrected, see Table 1.

*** Because the IRSL age constrains the age of the capping loess (Ql2) and the underlying alluvial gravel (Qg2) is 2 m deeper, these incision rates are maximum limiting and the actual incision rate may be less.

*** Maximum incision rate - the actual incision rate is probably lower because luminescence age provides only a lower bound to age of Qg4.

LIST OF FIGURES

Figure 1. A. Tectonic map of the Pacific northwest modified from Wells et al. (1998). Bold black arrows show the northern rotation of the fore-arc block relative to Penticton. White arrows, plate motion of the Juan de Fuca and Pacific plates relative to North American plate. White triangles, active Cascade volcanic arc. B. Hillshade basemap of Washington and northern Oregon overlain by Quaternary faults based on the USGS fault map database. Purple box delineates boundaries of Figure 2.

Figure 2. A 10-meter digital elevation model (DEM) of the northwestern sub-province of the Yakima Fold Belt, illustrating the Kittitas Valley, Manastash, Umtanum and Yakima ridges and lower Yakima River Canyon. Green box delineates study area. Purple and black lines indicate structural geometry and faults mapped by Washington State Department of Natural Resources. Red, yellow, maroon, and brown lines represent approximate ages of Quaternary faults within the field area and surrounding region (USGS Quaternary Fault Database). Blue lines represent the major drainage network. The ridgelines approximately define strike of anticline axes within the Yakima Fold Belt. The broadly defined western boundary of the Yakima Fold Belt is identified by the gradual transition from east-west or northwest-southeast ridges trends of the fold belt westward to the mountainous topography of the Cascade Range.

Figure 3. A 1m LiDAR slope map of Manastash ridge, northern range front and southwestern Kittitas Valley. Purple and green box represent the sub areas: northwest range front (Figure 7) and Yakima Canyon Entrance (Figure 9), respectively.

Figure 4. A. Histograms of pebble and cobble lithology from five different alluvial units. B. Histograms of degree of cobble roundness from five different alluvial units. As suggested by Waitt (1979), Spring and Shushuskin alluvial deposits represent sidestream tributary facies; modern and paleo-Yakima River alluvial deposits represent mainstream facies.

Figure 5. Regional stratigraphic column of the southwest Kittitas Valley modified from Smith (1988) delineating the relationship between the Columbia River Basalt Group and the Ellensburg Formation. Expanded table illustrates the Quaternary lithofacies employed within this study for the Manastash range front and lower Yakima River Canyon.

Figure 6. A. Geologic map of the northern range front of Manastash Ridge and the southern Kittitas Valley, central Washington. Contour interval 2 m. Yellow line represents the location of the seismic reflection imagery; yellow dots are the seismic station numbers. Bedrock mapping beyond the green and blue boxes, including the southwestern edge of cross section B-B', was adapted from the Yakima Quadrangle 1:100,000 scale geologic map (Washington Department of Natural Resources, 1978). B. Legend for the geologic map depicted in Figure 6A.

Figure 7. A. LiDAR (1 m resolution) slope map of the western range front of Manastash Ridge extending from Long Tom Canyon in the northwest to Benwy Canyon in the southeast. B. Companion geologic map of the western Manastash range front. See Figures 5 and 6 for unit and geologic symbol descriptions. Pebble and cobble count sample locations are

noted by black circles with blue centers. Modern Yakima River cobble count sample location is beyond the limits of the map. Red and yellow stars depict sample locations for IRSL and Tephra analyses. Contour interval 2 m.

Figure 8. Stratigraphic columns of Quaternary units within the west-of-the-canyon range front and Yakima River Canyon. A. Composite stratigraphic section near mouth of Spring Canyon, B. Composite stratigraphic section of strath terrace sequence Qg4/Qf4/Qlu in northern portion of abandoned meander, C. Composite stratigraphic section of strath terrace sequence Qg2 overlain by Ql2 in southern portion of abandoned meander.

Figure 9. A. LiDAR (1 m resolution) slope map of the Yakima Canyon entrance extending southward across Manastash ridge into the lower Yakima River Canyon. B. Companion geologic map of the canyon entrance and adjacent areas. Blue line represents the south flowing Yakima River. See Figures 4 and 6 for unit and geologic symbol descriptions. Red and yellow stars depict sample locations for IRSL and Tephra analyses. Contour interval 2 m.

Figure 10. Geologic cross sections, no vertical exaggeration. Cross section A-A' extends northwest from Manastash Ridge to Kitittas Valley within the vicinity of the Lower Yakima River Canyon entrance. Cross section B-B' extends northwest from Manastash Ridge to Kittitas Valley, adjacent to Shushuskin Canyon. Geologic units within the Ellensburg Formation (Figure 5): Tgr, Grand Ronde basalt member; Tev, Vantage clastic member; Tw, Wanapum basalt member; Tesc, Squaw Creek clastic member; Tue, Upper Ellensburg Formation.

Figure 11. A. Migrated seismic reflection imagery along Umtanum road. Seismic reflection line trends northwest within Shushuskin Canyon from stations 0 to 300 where extends from the incised valley onto the alluvial sediments changing orientation to due north between stations 300 to 700. B. Interpreted migrated seismic reflection imagery. Green lines represent bedding, red lines represent faults, yellow line delineates the transition between alluvial sediment and basalt.

Figure 12. A. Longitudinal profiles of the Manastash range front tributaries. Dashed lines represent tributaries situated in the eastern range front. B. Longitudinal profiles of Spring, Benwy and Noname canyons. Green boxes indicate corresponding knickpoints. Note coincident knickpoint elevations range at 510 m.

Figure 13. Slope-drainage area plots for the range front tributaries. All plots use raw slope and area data. For LiDAR-based DEMs, data extraction interval was 1 m. The one exception was the 10-m-DEM basis for the Shushuskin Canyon data, where the extraction interval was 12.41 m and the plots used a smoothing window of 250 m.

Figure 14. A. Longitudinal profile of Spring Canyon. B. Longitudinal profile of just the lower reach of Spring Canyon. Point elevations from each alluvial unit (Qf2, Qf3, Qf4) were projected horizontally onto the vertical plane containing the channel thalweg thereby

defining fan surface elevations above the tributary thalweg. Relict profile (dashed line) projected downstream from knickpoint to alluvial fan surface Qg4.

Figure 15. Cross Section extending from Manastash range front northward to Potato Hill within the southern Kittitas Valley. Teu, Upper Ellensburg Formation; Tth, Thorp gravel of Waitt (1979); Qf, Quaternary fan deposit.

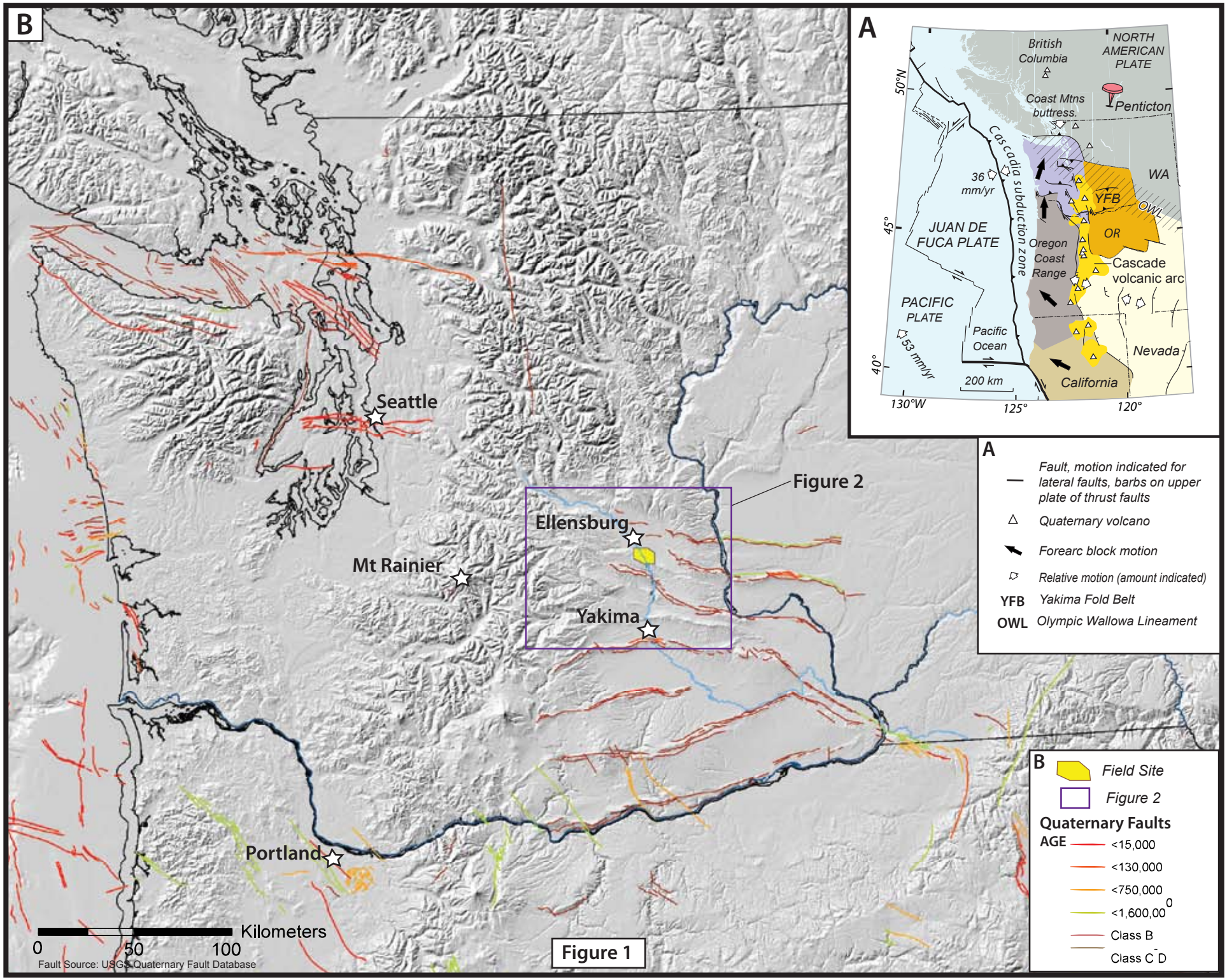
B
A
British Columbia
NORTH AMERICAN PLATE
Coast Mtns buttress.
Penticton
50°N
Cascadia subduction zone
36 mm/yr
WA
YFB
OWL
45°
JUAN DE FUCA PLATE
OR
Oregon Coast Range
Cascade volcanic arc
PACIFIC PLATE
Pacific Ocean
53 mm/yr
Nevada
40°
200 km
California
130°W
125°
120°
Seattle
Figure 2
Ellensburg
Mt Rainier
Yakima
Portland
Kilometers
0
50
100
Fault Source: USGS Quaternary Fault Database
Figure 1
A
Fault, motion indicated for lateral faults, barbs on upper plate of thrust faults
Quaternary volcano
Forearc block motion
Relative motion (amount indicated)
YFB Yakima Fold Belt
OWL Olympic Wallowa Lineament
B
Field Site
Figure 2
Quaternary Faults
AGE
<15,000
<130,000
<750,000
<1,600,000
Class B
Class C D

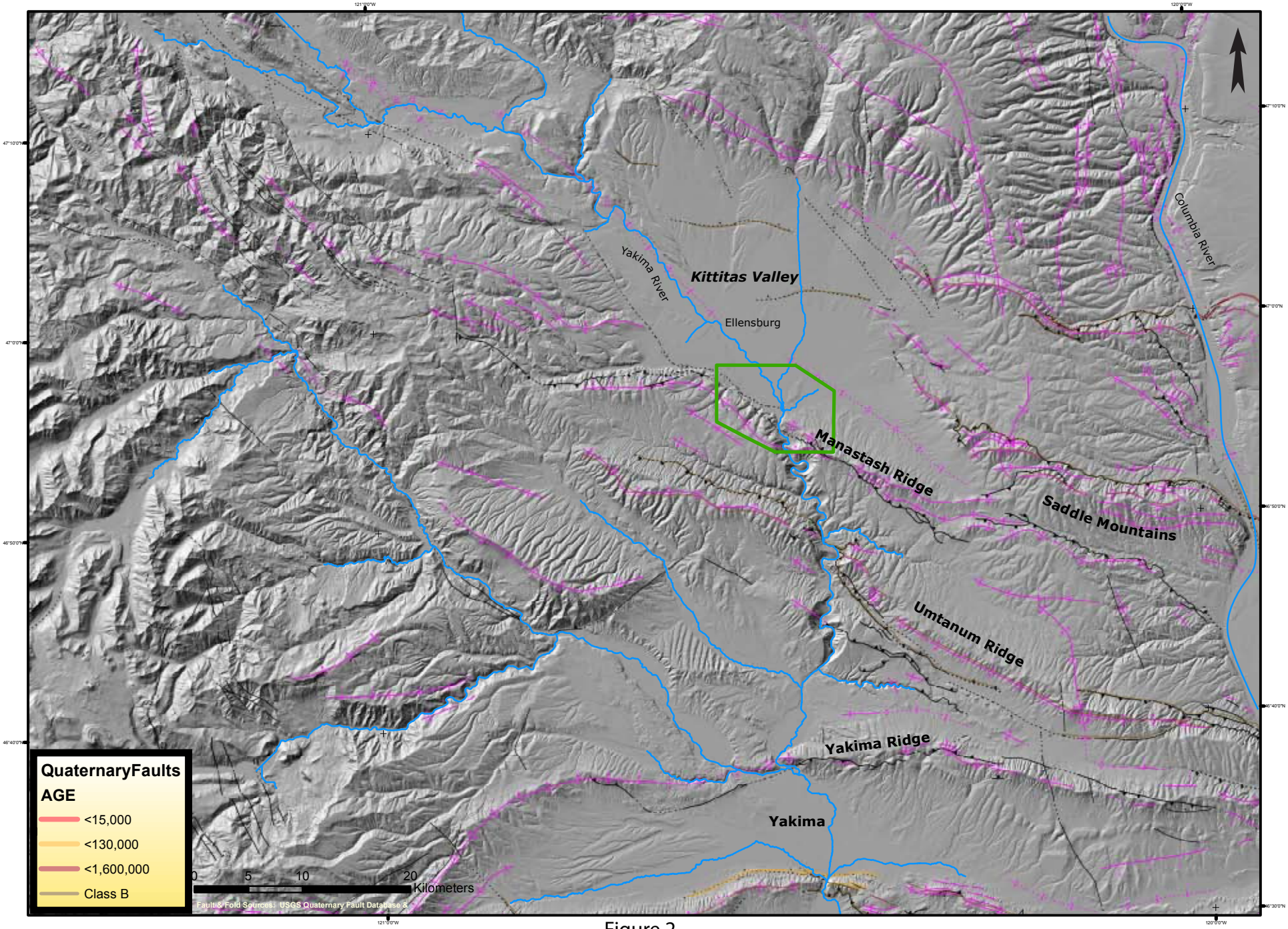
Kittitas Valley
Ellensburg
Yakima River
Columbia River
Manastash Ridge
Saddle Mountains
Umtanum Ridge
Yakima Ridge
Yakima
QuaternaryFaults
AGE
<15,000
<130,000
<1,600,000
Class B
0 5 10 20
Kilometers
Fault & Fold Sources: USGS Quaternary Fault Database &

Figure 2

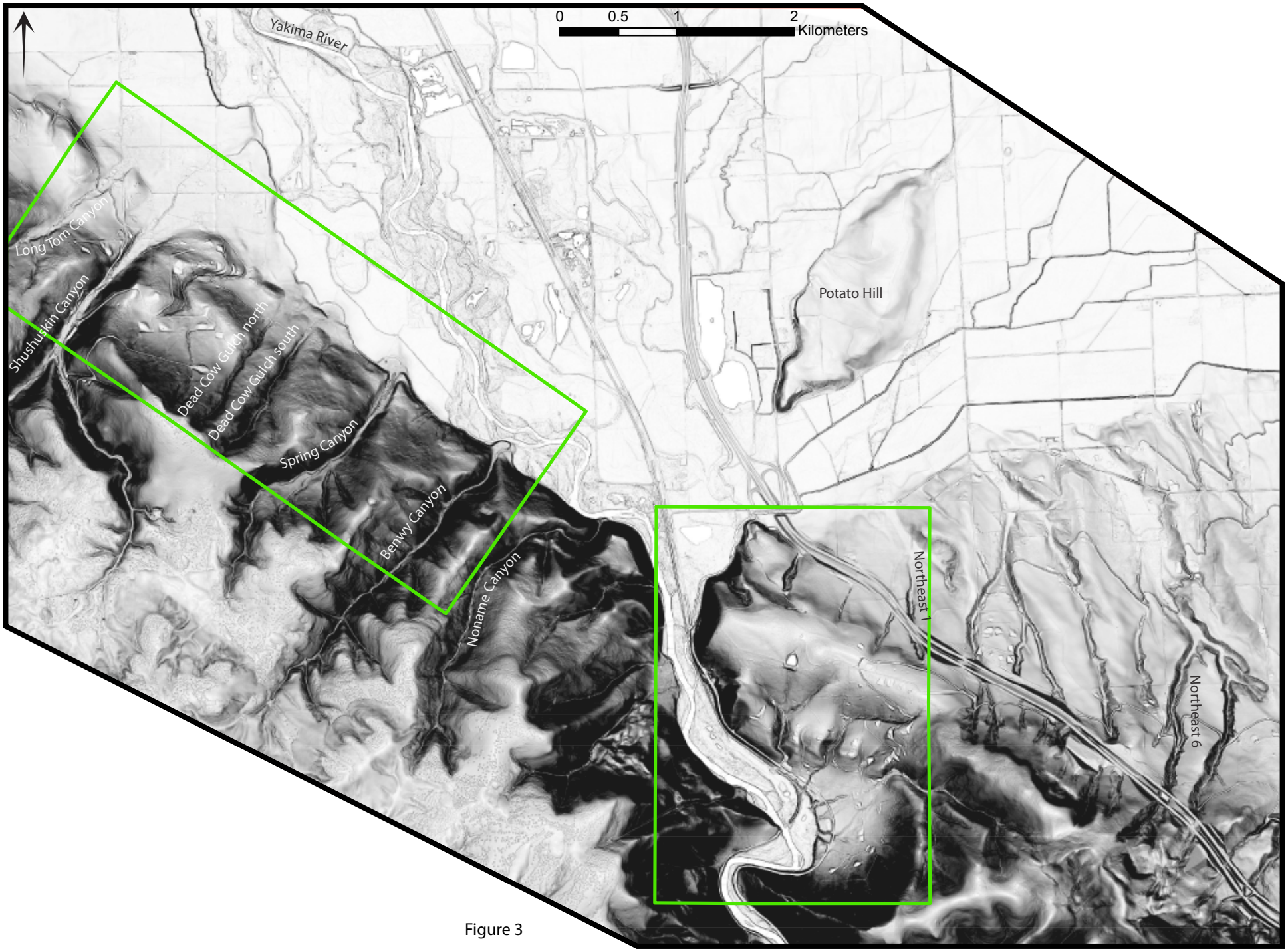
0
0.5
1
2
Kilometers
Yakima River
Long Tom Canyon
Shushuskin Canyon
Dead Cow Gulch north
Dead Cow Gulch south
Spring Canyon
Benwy Canyon
Noname Canyon
Potato Hill
Northeast 1
Northeast 6

Figure 3

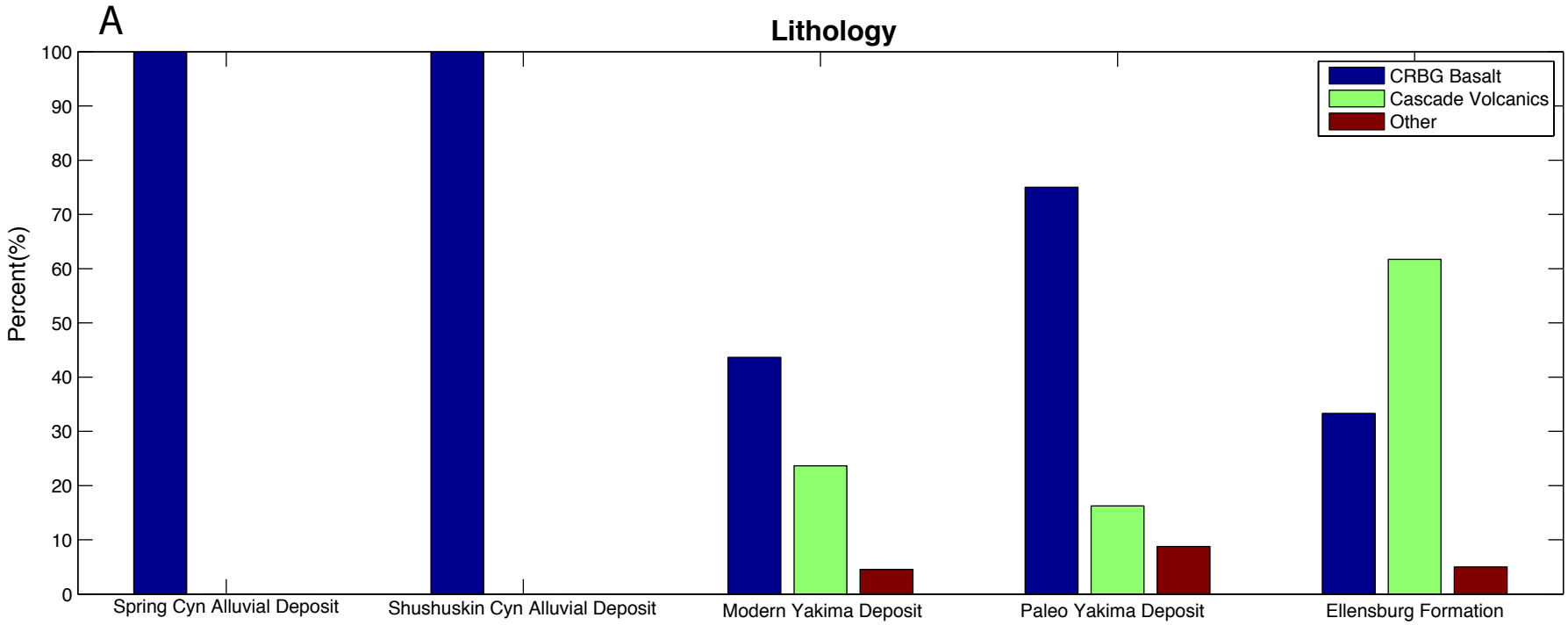
A
Lithology
Percent(%)
0
10
20
30
40
50
60
70
80
90
100
CRBG Basalt
Cascade Volcanics
Other
Spring Cyn Alluvial Deposit
Shushuskin Cyn Alluvial Deposit
Modern Yakima Deposit
Paleo Yakima Deposit
Ellensburg Formation

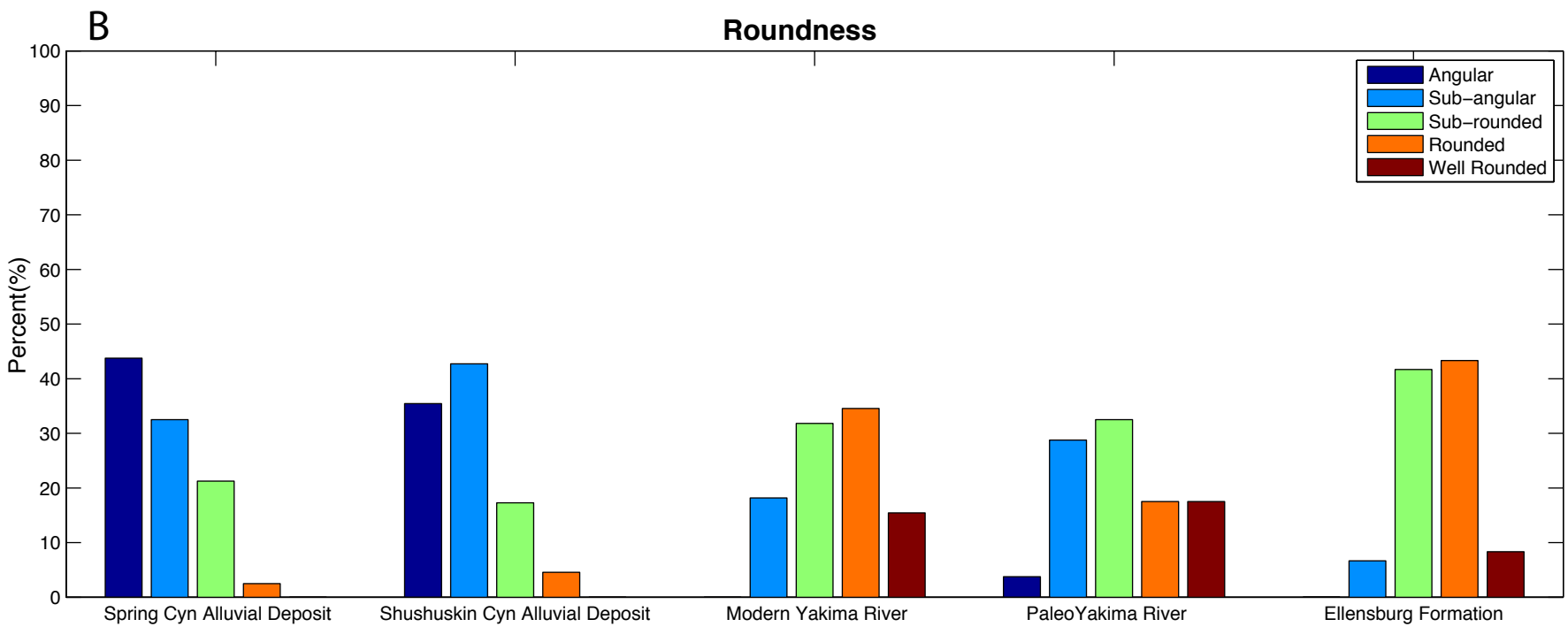
B
Roundness
Percent(%)
0
10
20
30
40
50
60
70
80
90
100
Angular
Sub−angular
Sub−rounded
Rounded
Well Rounded
Spring Cyn Alluvial Deposit
Shushuskin Cyn Alluvial Deposit
Modern Yakima River
PaleoYakima River
Ellensburg Formation

Figure 4

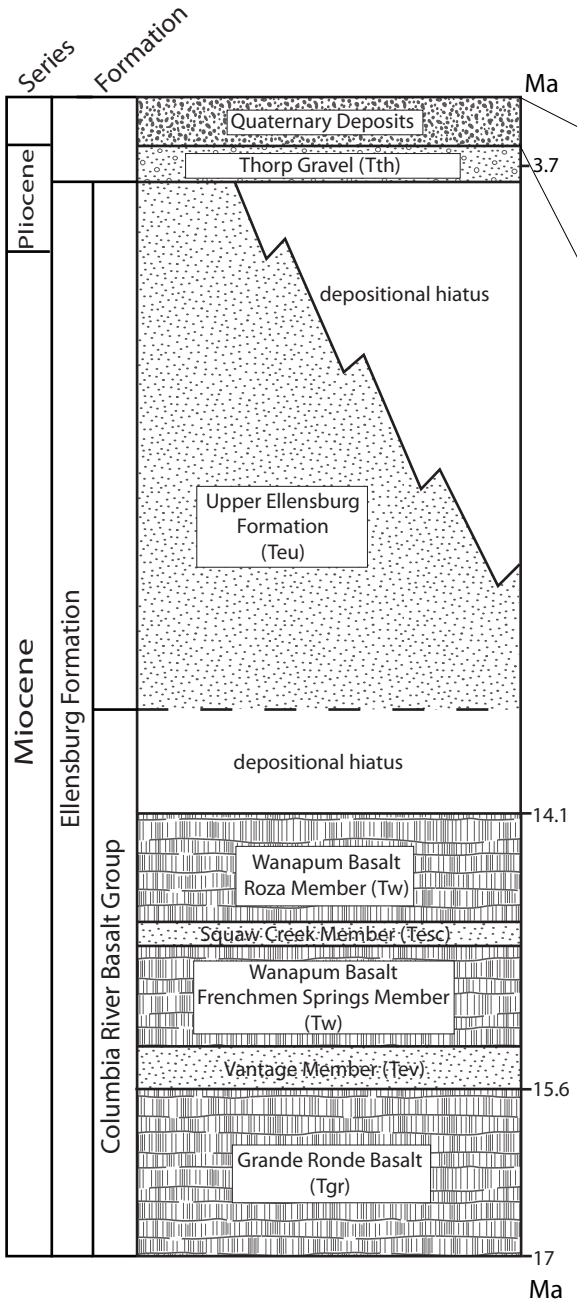

Quaternary deposits in the vicinity of Manastash Ridge range-front and Entrance to lower Yakima River Canyon

← Increasing Relative Age	**Yakima River alluvium** "Mainstream" facies of Waitt (1979)		**Tributary fan alluvium** "Sidestream" facies of Waitt (1979)		**Undifferentiated alluvial Deposits**	**Loess**		**Landslide Deposits**
	Modern alluvium	Qal	Modern alluvium	Qal				
	Holocene alluvium	Qoal	Modern fan deposits	Qf1				
	Alluvial terrace Gravels (Pleistocene)	Qg2	Older fan deposits (Late Pleistocene)	Qf2	Qfu	Ql2	Qlu	Qls
				Qf3				
		Qg4		Qf4				
		Qg5		Qf5				
		Qg6		Qf6				
				Qf7				

Figure 5

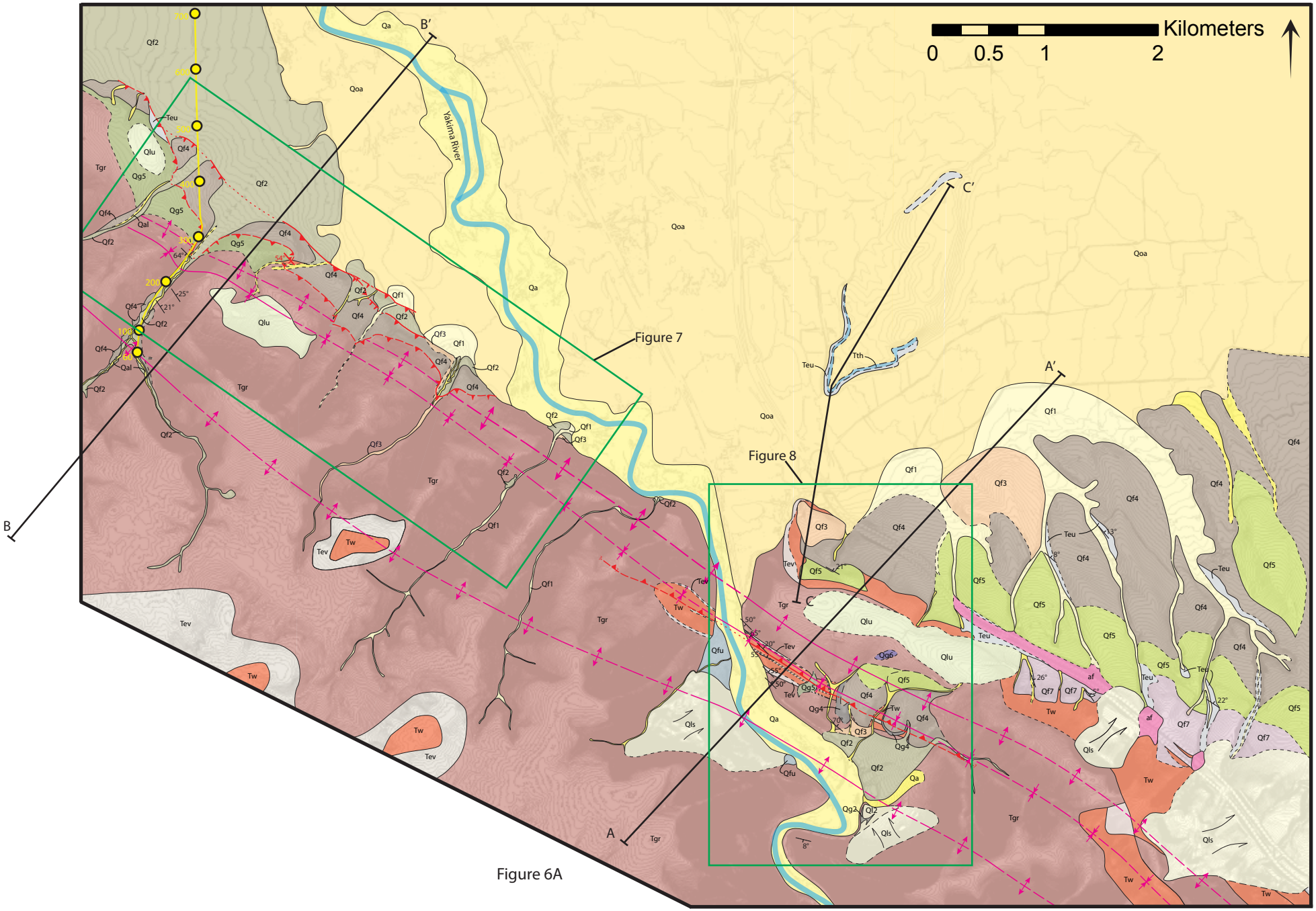
Kilometers
0
0.5
1
2
Yakima River
Figure 7
Figure 8
A
A′
B
B′
C
C′
Qa
Qoa
Qf1
Qf2
Qf3
Qf4
Qf5
Qf7
Qg5
Qg4
Qg6
Qlu
Qls
Qfu
Qal
Tgr
Tev
Tw
Teu
Tth
af

Figure 6A

Geologic Symbols

contact; solid where observed; dashed where approximated/concealed

reverse Fault; solid where observed; dashed where approximated/concealed

syncline; solid where observed; dashed where approximated/concealed

anticline; solid where observed; dashed where approximated/concealed

54° Fault Orientations

21° Bedding Attitudes

600 700 seismic reflection line with station number

Geologic Units

- af — artificial fill
- Qa — Modern Yakima River Alluvium
- Qal — Modern Alluvium
- Qoa — Older Yakima River Alluvium
- Qls — Quaternary Landslide Deposit
- Qf1 — Quaternary Fan Deposit 1
- Ql2 — Quaternary Loess Deposit 2
- Qf2 — Quaternary Fan Deposit 2
- Qg2 — Quaternary paleo-Yakima River gravels 2
- Qf3 — Quaternary Fan Deposit 3
- Qf4 — Quaternary Fan Deposit 4
- Qg4 — Quaternary paleo-Yakima River gravel 4
- Qf5 — Quaternary Fan Deposit 5
- Qg5 — Quaternary paleo-Yakima River gravel 5
- Qg6 — Quaternary paleo-Yakima River gravel 6
- Qf7 — Quaternary Fan Deposit 7
- Qlu — Quaternary Loess Undifferentiated
- Qfu — Quaternary Fan Deposits Undifferentiated
- Tth — Thorp Gravels
- Teu — Upper Ellensburg Formation
- Tw — Columbia River Basalt Group, Wanapum
- Tesc — Ellensburg Formation, Squaw Creek Member
- Tev — Ellensburg Formation, Vantage Member
- Tgr — Columbia River Basalt Group, Grand Ronde

Figure 6B

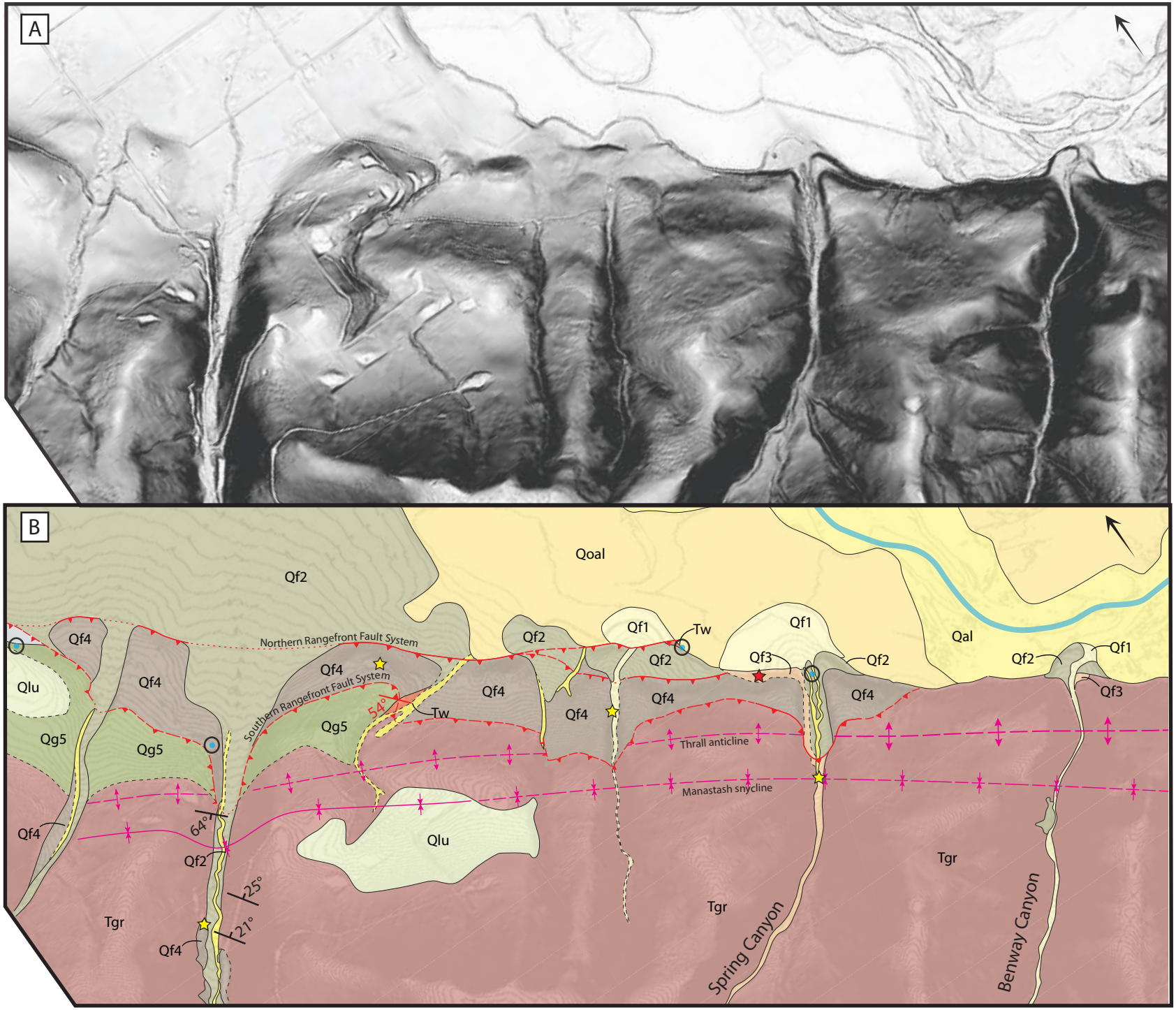
A
B
Qoal
Qf2
Qf1
Tw
Qf3
Qal
Qf4
Qlu
Qg5
Northern Rangefront Fault System
Southern Rangefront Fault System
54°
64°
25°
21°
Thrall anticline
Manastash snycline
Tgr
Spring Canyon
Benway Canyon
IRSL Sample Locations
Tephra Sample Locations
Pebble and Cobble Count Locations
0
1km

Figure 7

A

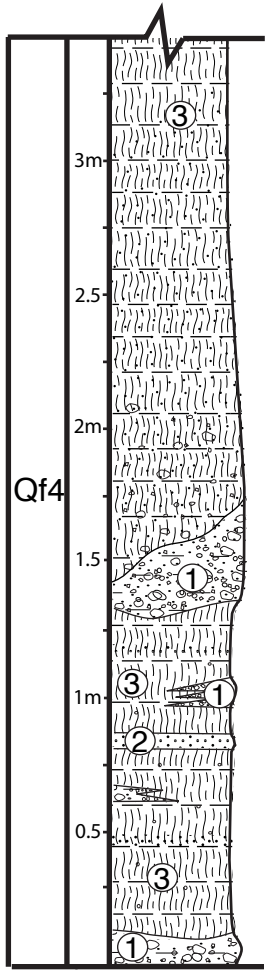

1. Distal Fan Deposit; pebble and small cobble; 1cm to 10cm diameter; angular to sub-rounded; clast supported; sidestream basalt lithology. Unit thickness varies from 10 to 40cm; thin exposures are not laterally continuous.

2. Alluvial Sand; pebble and granule-grained interbed, 2-5 cm thick.

3. Loess; intercalated with fine to coarse-grained sand; moderately indurated; few pebbles; small to large blocky peds; common medium to coarse-grained-sand and pebble interbeds. Fine-grained sand increasing in dominance grading up section.

B

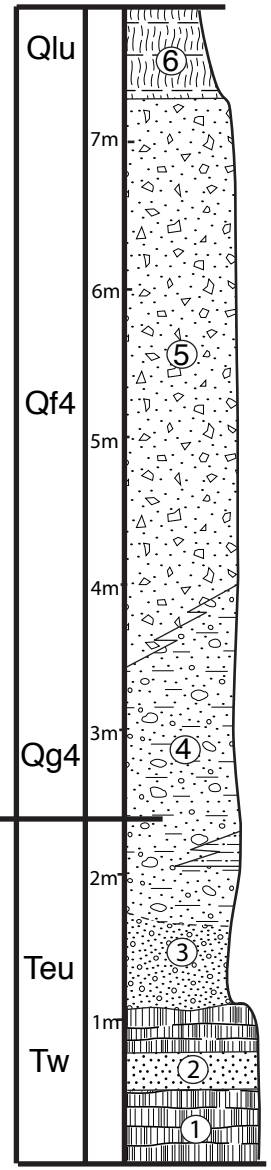

1. Wanapum Basalt Member; vecsiculated flow top; bedding wavy and indistinct.

2. Sandstone interbed, thin (0.2 to 0.4m); poorly cemented.

3. Ellensburg Conglomerate; 0.5 to 10cm diameter thick, predominately 1 to 5cm diameter; well sorted; sub-rounded to well rounded; abundant Cascade-derived lithics; clast supported.

4. Paleo-Yakima River Gravels; sub-angular to rounded pebbles; increasing fequencey of basalt lithology; matrix supported, medium to coarse-grained. Interbedded with 20 - 30 cm thick alluvial siltstone with common pebbles of mixed lithology.

5. Alluvial Fan Deposit 4; angular to sub-angular cobbles, predominately basalt lithology; matrix supported, medium-grained sand with common pebbles. Matrix grades upward to fine-grained sand.

6. Loess; yellowish brown silty loess, poorly consolidated with few pebbles and granules

C

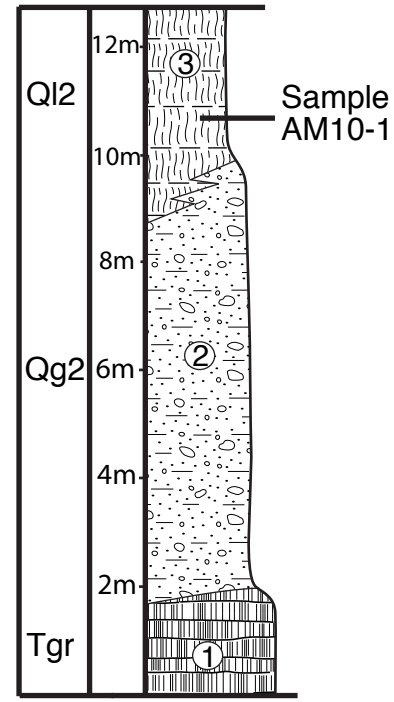

3. Loess; light yellowish brown; sandy loess, poorly to moderately developed peds, upper 2 meters unconsolidated.

2. Paleo-Yakima River gravel (Qg2); sub-angular to rounded pebbles; matrix supported, fine to coarse-grained sand. Mixed lithologies

1. Basalt, Grand Ronde Member

Figure 8

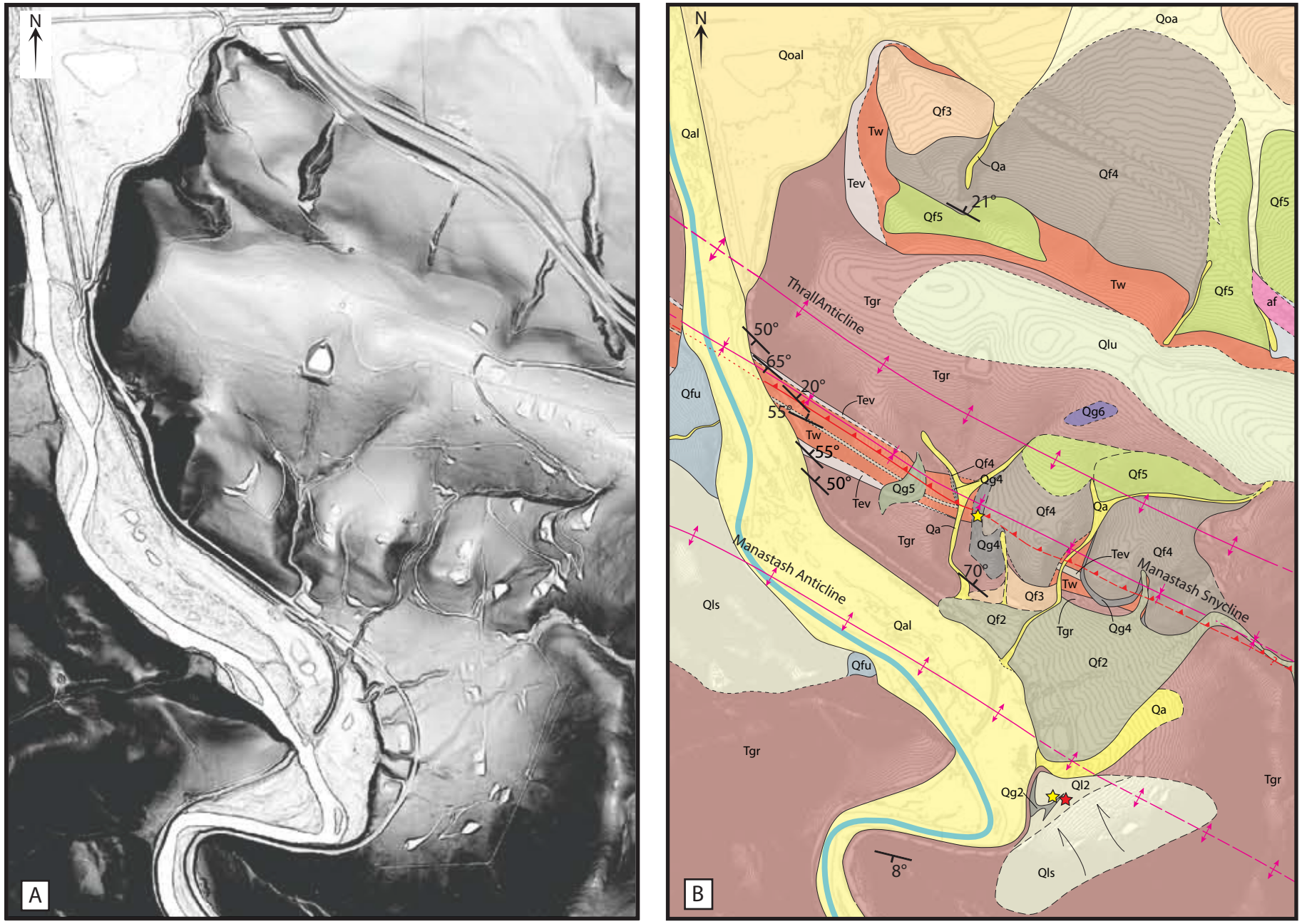

0 1km

Figure 9

IRSL Sample Locations

Tephra Sample Locations

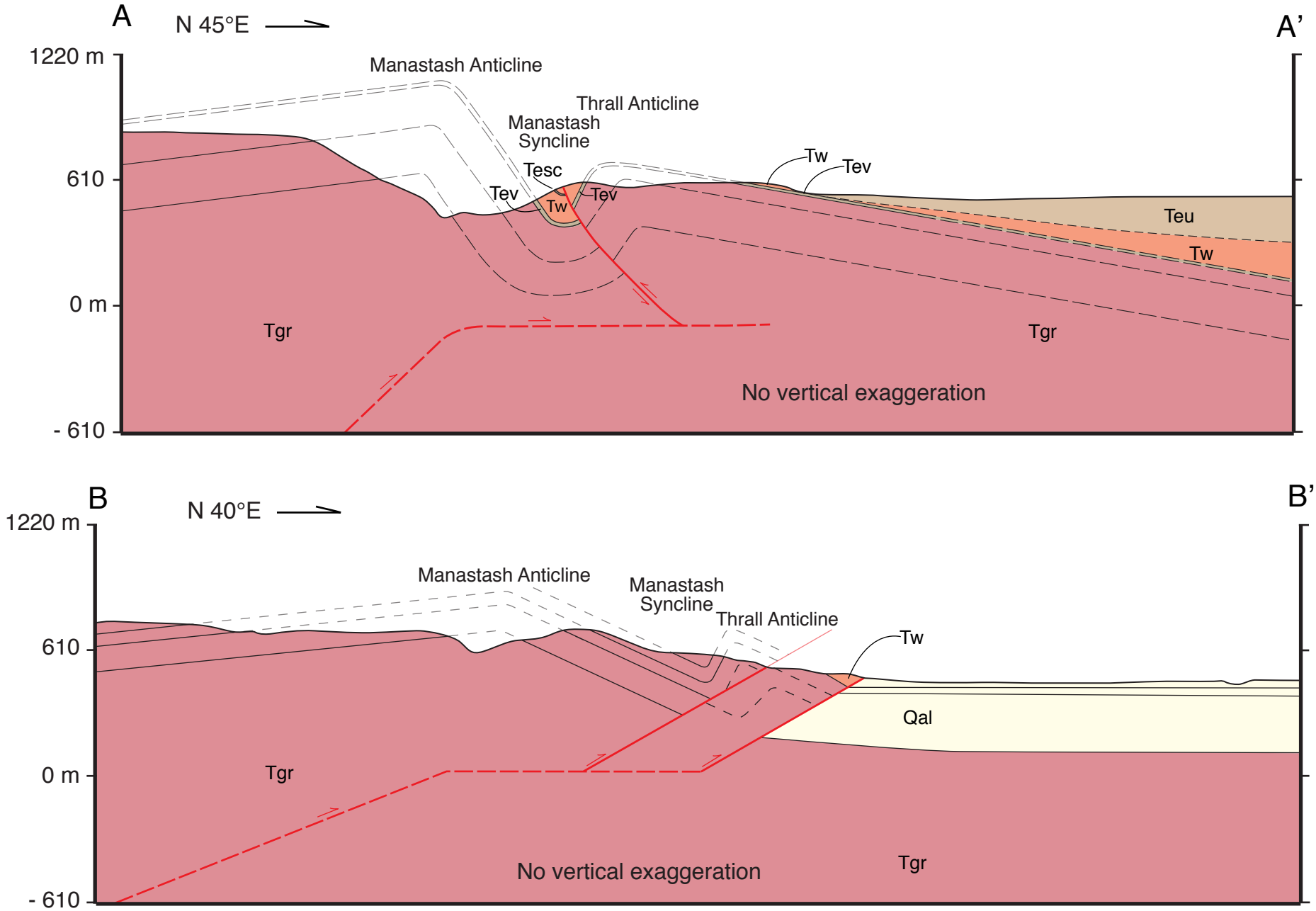
A
N 45°E
A'
1220 m
610
0 m
- 610
Manastash Anticline
Thrall Anticline
Manastash
Syncline
Tesc
Tev
Tw
Tev
Tw
Tev
Teu
Tw
Tgr
Tgr
No vertical exaggeration
B
N 40°E
B'
1220 m
610
0 m
- 610
Manastash Anticline
Manastash
Syncline
Thrall Anticline
Tw
Qal
Tgr
Tgr
No vertical exaggeration

Figure 10

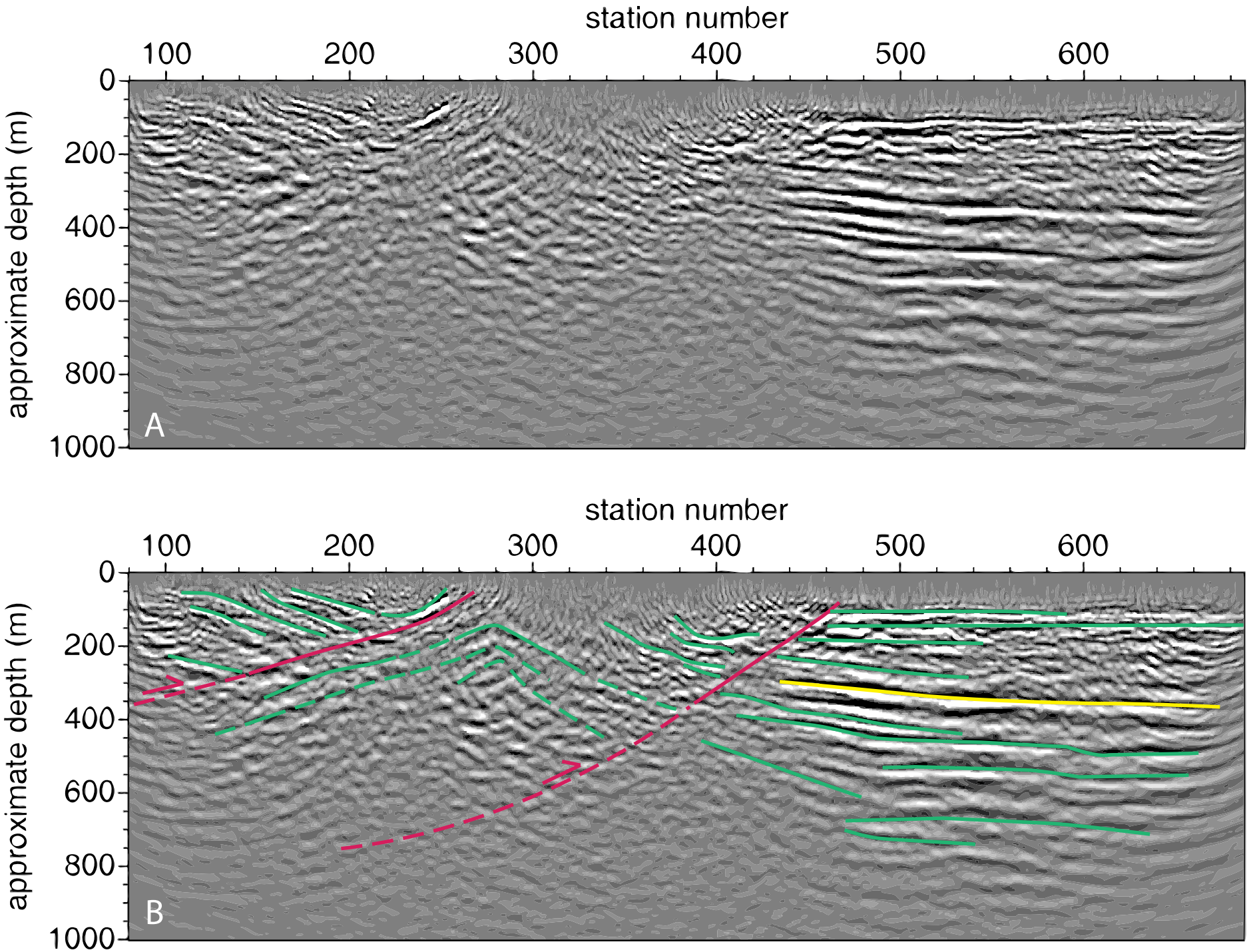
station number
100
200
300
400
500
600
0
200
400
600
800
1000
approximate depth (m)
A
station number
100
200
300
400
500
600
0
200
400
600
800
1000
approximate depth (m)
B

Figure 11

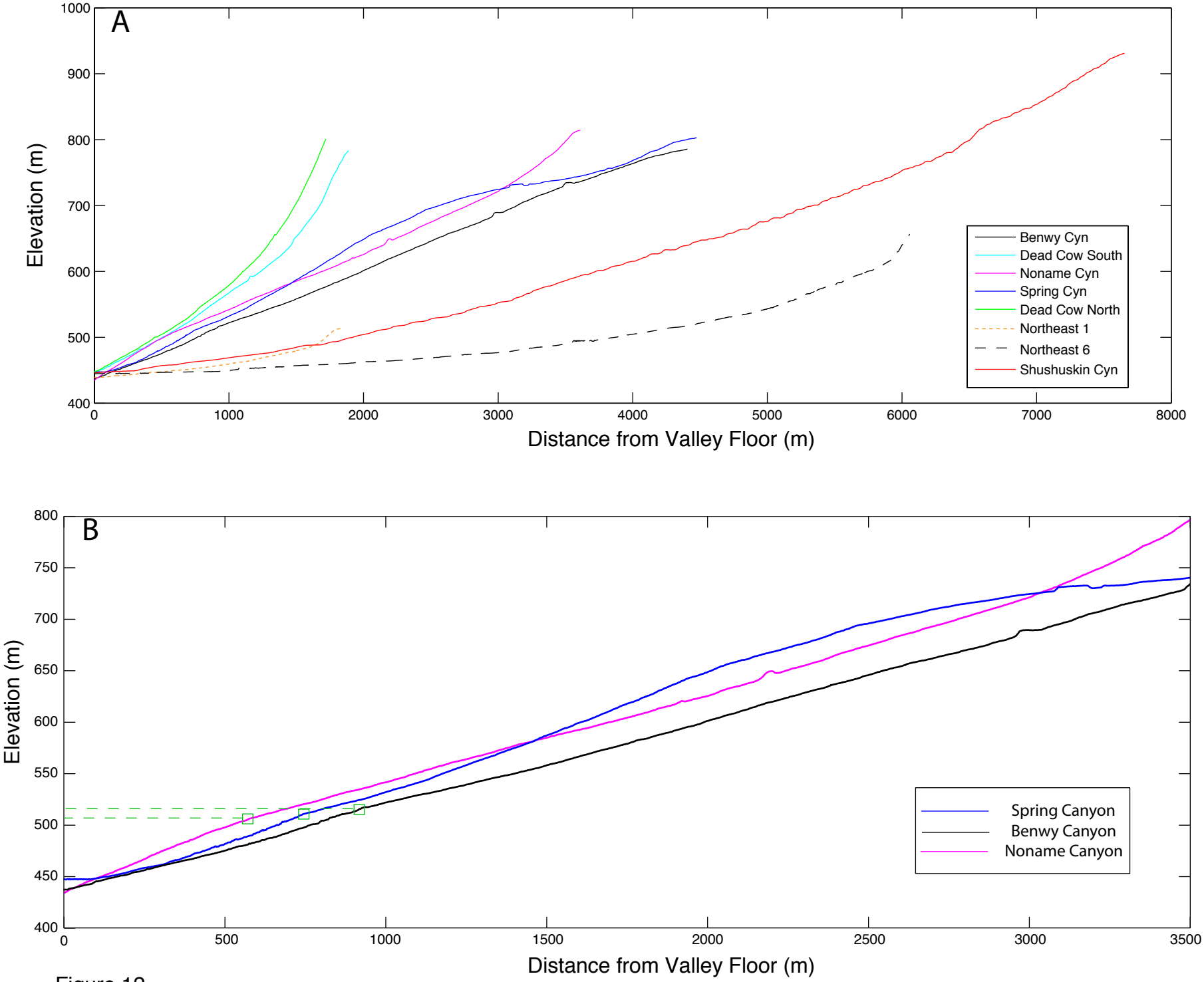
A
Elevation (m)
Distance from Valley Floor (m)
Benwy Cyn
Dead Cow South
Noname Cyn
Spring Cyn
Dead Cow North
Northeast 1
Northeast 6
Shushuskin Cyn
B
Elevation (m)
Distance from Valley Floor (m)
Spring Canyon
Benwy Canyon
Noname Canyon

Figure 12

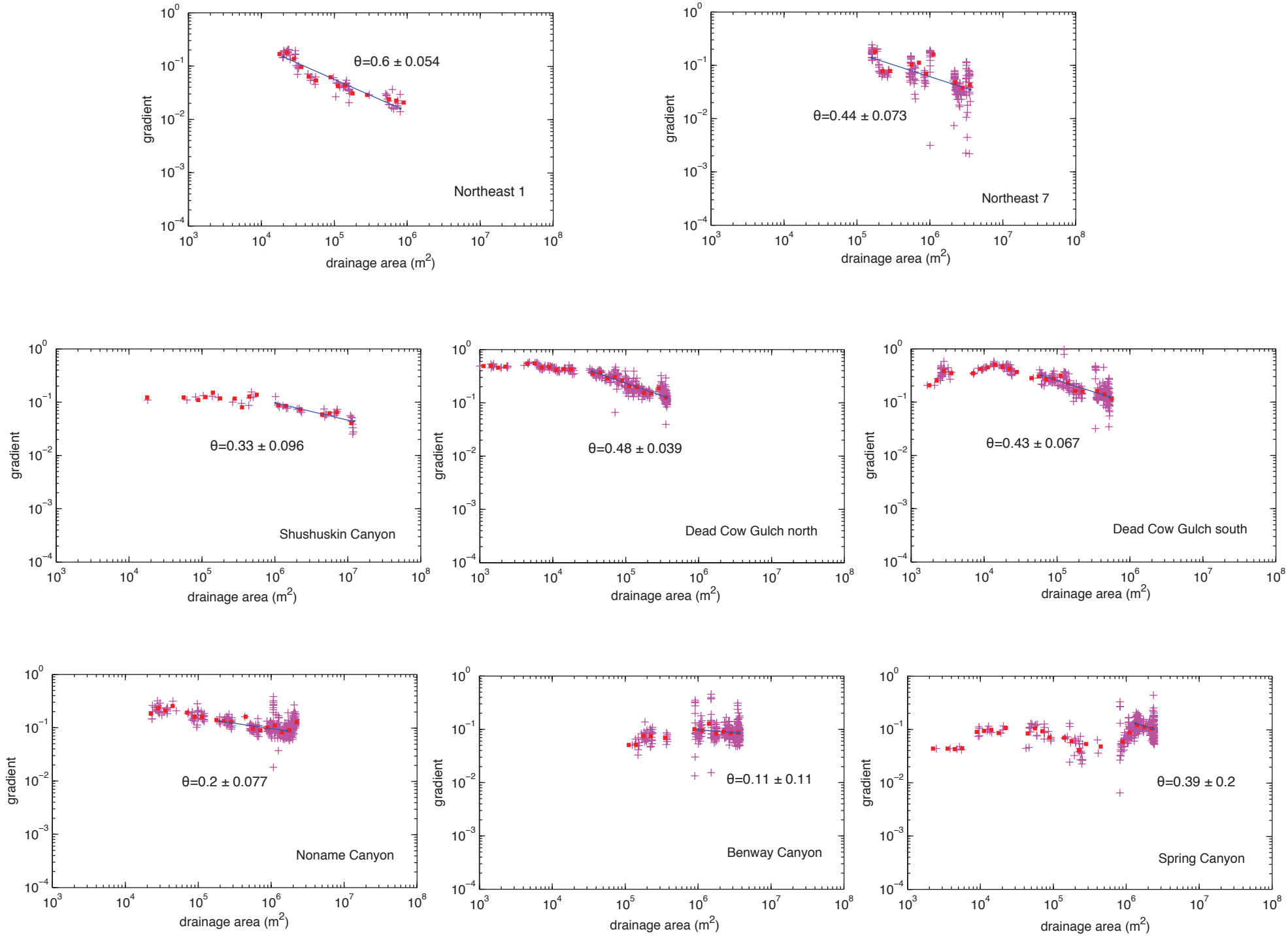
θ=0.6 ± 0.054
Northeast 1
θ=0.44 ± 0.073
Northeast 7
θ=0.33 ± 0.096
Shushuskin Canyon
θ=0.48 ± 0.039
Dead Cow Gulch north
θ=0.43 ± 0.067
Dead Cow Gulch south
θ=0.2 ± 0.077
Noname Canyon
θ=0.11 ± 0.11
Benway Canyon
θ=0.39 ± 0.2
Spring Canyon
gradient
drainage area (m2)

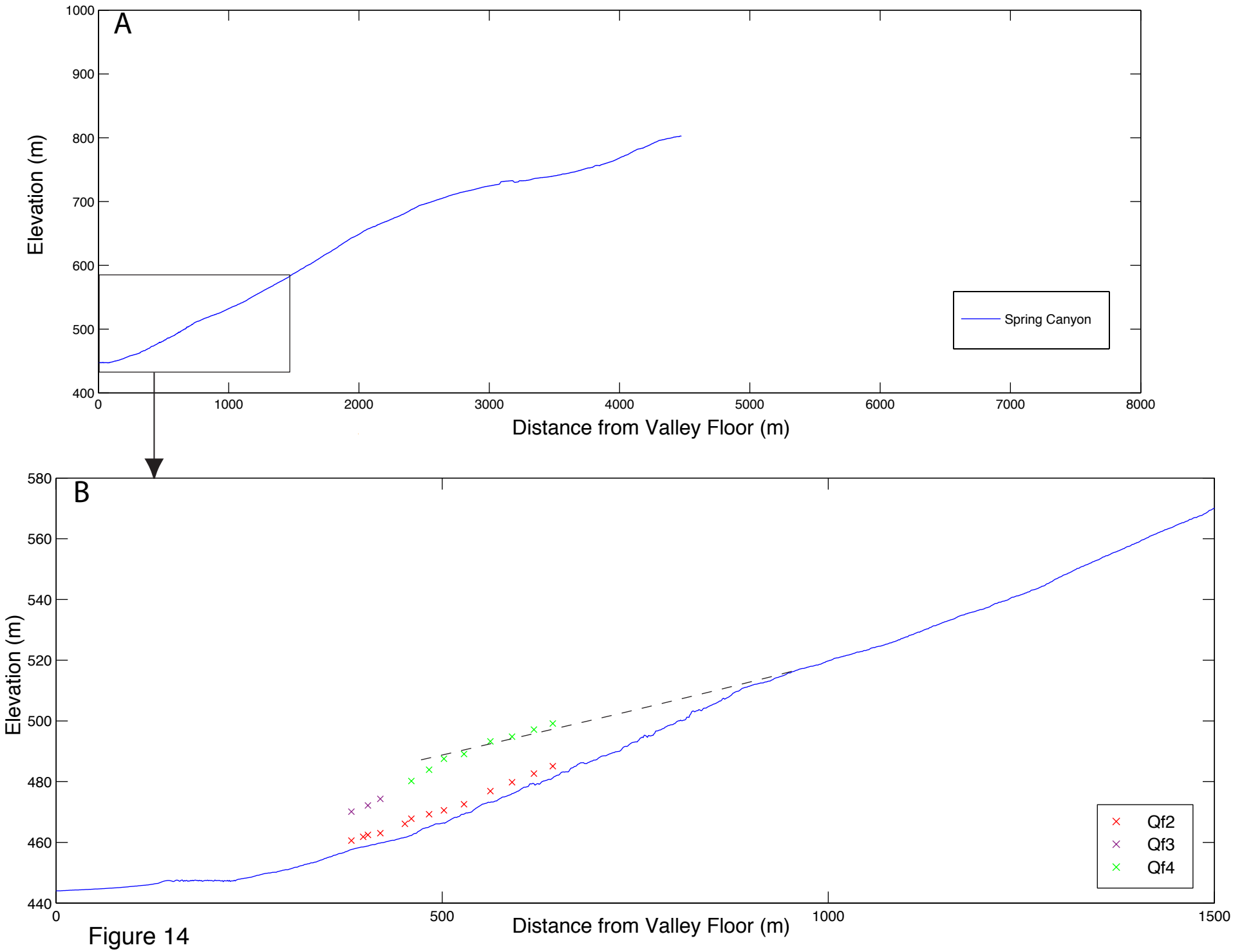
A
Elevation (m)
Distance from Valley Floor (m)
Spring Canyon
B
Elevation (m)
Distance from Valley Floor (m)
Qf2
Qf3
Qf4

Figure 14

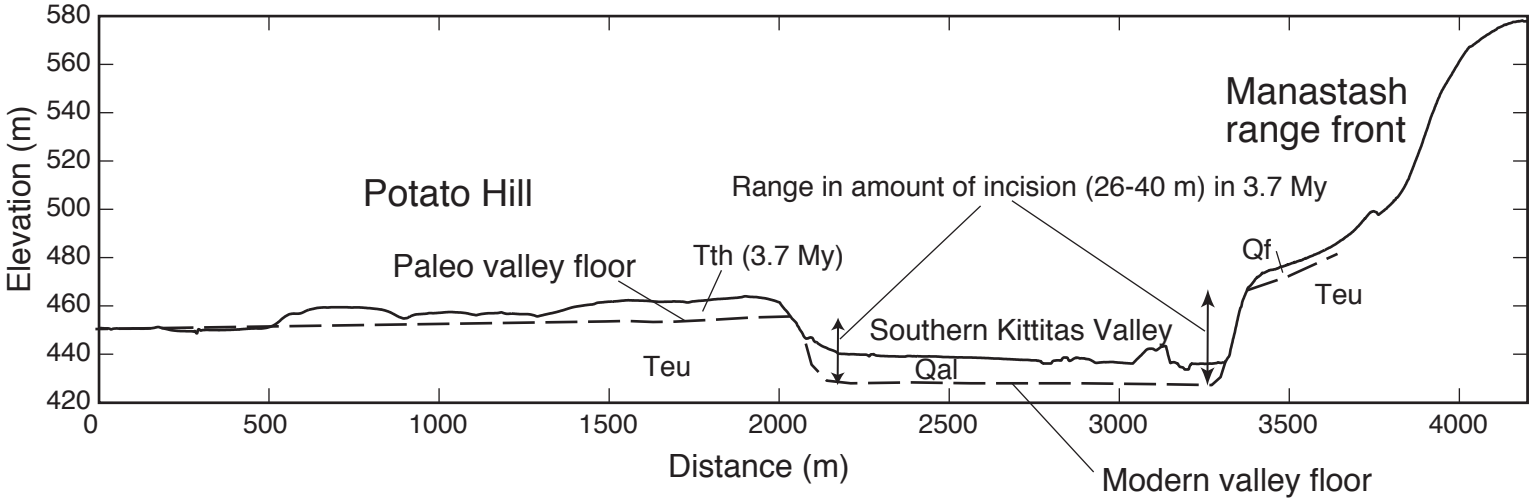
580
560
540
520
500
480
460
440
420
Elevation (m)
0
500
1000
1500
2000
2500
3000
3500
4000
Distance (m)
Manastash
range front
Potato Hill
Range in amount of incision (26-40 m) in 3.7 My
Paleo valley floor
Tth (3.7 My)
Qf
Teu
Southern Kittitas Valley
Teu
Qal
Modern valley floor

Figure 15